COMMONALITIES OF AXONAL REPAIR: UNDERSTANDING TRACT DIVERSITIES & MOLECULES INVOLVEMENT

Charlène Marguerite Joséphine Granier

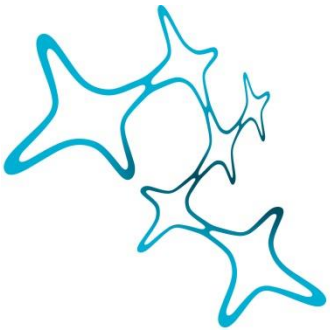

Graduate School of Systemic Neurosciences

LMU Munich

Dissertation der
Graduate School of Systemic Neurosciences
Ludwig-Maximilians-Universität München

January 2021

Supervisor
Dr Florence Bareyre
Institute for Clinical Neuroimmunology
LMU Munich

First Reviewer: Dr Florence Bareyre
Second Reviewer: Dr Jovica Ninkovic
External Reviewer: Dr Radika Pattagunta

Date of Submission: January 19, 2021
Date of Defense: June 9, 2021

A toi Laura si tu me regardes

Tout a commencé quand tu es parti et

aujourd´hui encore tu me guides

Index

List of abbreviations

AAV	Adeno-associated virus
AD	Autonomic Dysreflexia
AIS	ASIA Impairment Scale
ASIA	American Spinal Injury Association
BBB	Basso, Beattie and Bresnahan
CGRP	Calcitonin gene-related peptide
CST	Corticospinal tract
DRG	Dorsal root ganglion
EGFP	Enhanced green fluorescent protein
EYFP	Enhanced yellow fluorescent protein
FGF	Fibroblast growth factor
GABA	Gamma aminobutyric acid
GAD	Glutamate decarboxylase
GlyT2	Glycinergic Transporter 2
LPSN	Long propriospinal neuron
MP	Methylprednisolone
PV	Parvalbumine
SCI	Spinal Cord Injury
STAT3	Signal transducer and activator of transcription 3
TM	Tirilazad Mesylate
USA	United States of America

Abstract

There was in 2019 in the USA alone over 17 000 new cases of spinal cord injury and close to 300 000 patients in total. This life-threatening condition isn't only traumatic and devastating for patients and their family, it is as well an enormous financial burden. Patients suffering spinal cord injury will lose the ability to move and feel below the level of the injury, making them either paraplegic or tetraplegic. Complete lesions, where no tissue is spared will impair the patient for life with no chance of recovery without medical intervention. Even if incomplete lesions leave the possibility of some level of recovery, the path is long and sometimes unsuccessful. This recovery was shown to rely on remodeling of cut axons away from the scar tissue in both motor and sensory systems. In order to reach recovery, the cut axons will have to sprout and reach a suitable target, that will then convey the inputs previously lost. The motor pathways have been studied for decades because of their prevalence and importance in injured patients, but always more reports inform on the necessity to recover both motor and sensory inputs in order to regain full motricity.

The purpose of this thesis was to look how sensory axons remodel following dorsal column lesion and if, like in the motor system, formation of a detour circuit allowed functional recovery.

First, we investigated how DRG axons remodel following dorsal column lesion and observed significant increase in DRG sprouting in the grey matter of the spinal cord 3 weeks after injury persisting at 12 weeks. When we looked at the localization of DRG

collaterals, we saw an increase of boutons in the dorsal and ventral layers of the spinal cord, leading to the search and discovery of DRG neurons' target: the cuneate nucleus projecting neurons. The study of contacts between DRG and cuneate nucleus projecting neurons showed an increase of contacts 3 weeks post lesion of DRG collaterals on cuneate nucleus projecting neurons as well as an overall increase of number of contacts onto single neurons at both 3 and 12 weeks.

Then, the characterization of these relay neurons presented new insights on possible molecular cues implicated in recovery in sensory tracts as an increase in contact onto parvalbumine and glutamate expressing cuneate nucleus neurons was found.

Finally, study of the spontaneous recovery using behavioral testing showed recovery of proprioceptive inputs 3 weeks after dorsal column lesion, validated by a relesion experiment.

To summarize, with this thesis, we aimed to better understand the detour circuit formation in the sensory system following dorsal column lesion. The characterization of the relay neurons might allow to find a therapeutic target for patients lacking sensory recovery.

Chapter 1 Introduction

I. Spinal cord injury (SCI) facts and figures

A spinal cord injury - damage to any part of the spinal cord or nerves at the end of the spinal canal - often causes permanent changes in strength, sensation and other body functions below the site of the injury (Mayo Clinic Staff, 2017). Only in Europe, the incidence of SCI goes from 5.5 to 195.4 cases per million (Jazayeri *et al*, 2015). Worldwide, it accounts for 23.0 cases per million on average, meaning about 7 500 new cases per year (Figure 1).

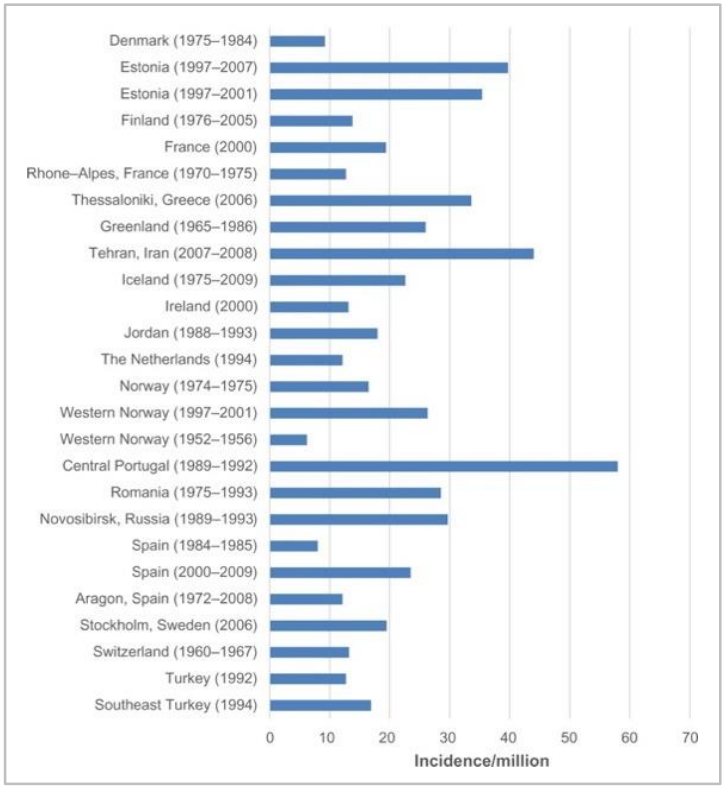

Figure 1 ***Annual incidence of spinal cord injury in regions and countries in Europe and the Middle East*** *(reprint permission from (Singh et al, 2014))*

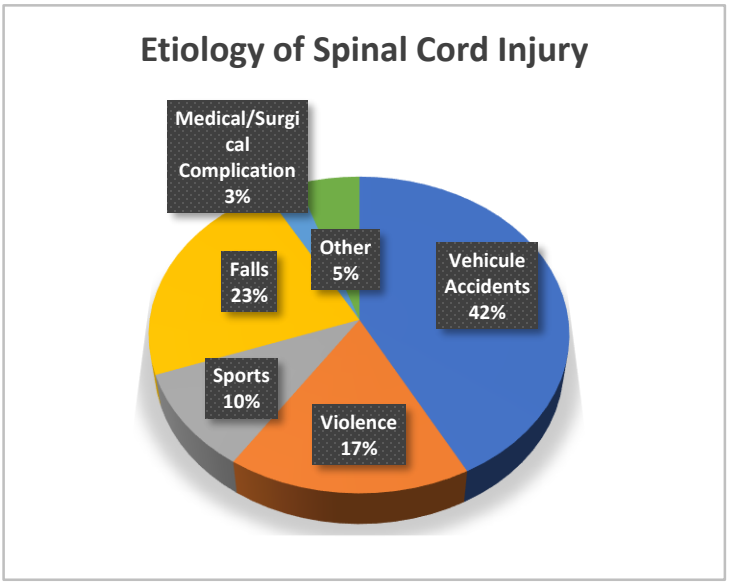

Figure 2 ***Etiology of Spinal Cord Injury*** *(graph of data from National Spinal Cord Injury Statistical Center)*

Most cases of SCI happen in males (78%) with an average age of 43 years old. Vehicle accidents and falls are at the moment accounting for 2/3 of the overall causes with 42 and 23% respectively (Figure 2).

In addition of being a tremendous change in a person's life, SCI patients have to deal with expensive and long-term costs (health care, living expenses, home upgrade, …). These costs highly depend on the severity and level of the injury but as well on the education, the pre-injury employment, or the neurological impairment (National Spinal Cord Injury Statistical Center, University of Alabama at Birmingham). For example, the first-year expenses of a patient suffering from a SCI at cervical level can reach 1,000,000 USD. Lifetime costs of such a 25-year-old patient would reach 4,000,000 USD by death time.

A spinal lesion leads to the loss of motor and sensory functions under the level of the injury. Different parameters define the impairment (Kirshblum *et al*, 2011) : a tetraplegia (or quadriplegia) refers to the loss of input from the cervical level, leaving the patient

without legs, arms and torso functions. A paraplegia refers to the loss of input from the thoracic, lumbar or sacral level, sparing the arms functions. A more precise scale has been used for years, the ASIA impairment scale (AIS), and defines the degree of impairment using five grades (Figure 3). Incomplete tetraplegia is the most occurring (with about 47% of the total SCI) followed by complete and incomplete paraplegia (with both 20% of the occurrence).

After an incomplete injury some degree of spontaneous recovery can be observed (Burns *et al*, 1997) and allow the patient to regain part of their motor and sensory functions (Raineteau & Schwab, 2001). Or the contrary, complete injuries have repercussions on the body far greater than the spinal lesion (Castro *et al*, 2000; Cramer *et al*, 2005) and lead to long term complications such as pressure ulcers or pneumonia (McKinley *et al*, 1999).

Hospitalizations have for the past 10 years greatly decreased due to the advanced of care and the causes of death after spinal cord injury have shift from septicemia to circulatory causes (Savic *et al*, 2017; Soden *et al*, 2000). Nevertheless, respiratory infections (pneumonia and bronchopneumonia) are still the main source of death with about 30% of the overall causes.

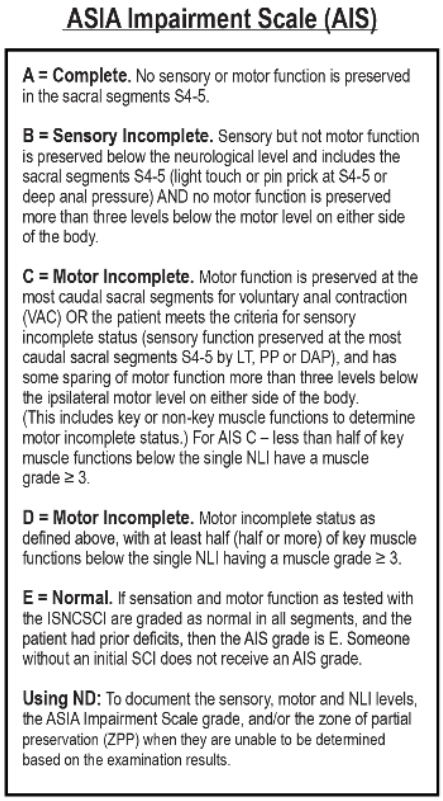

Figure 3 ***ASIA Impairment Scale*****©** *2011 American Spinal Injury Association. Reprinted with permission.*

II. Spinal cord injury pathophysiology

During and after spinal cord injury, two phases can be distinguished: the primary and the secondary phase (Figure 4).

The primary phase starts at the moment of the injury itself and include the impact and the following compression. The lesion to the spinal cord can result from various causes such as an impact, a laceration, a shear, … and involve four mechanisms: impact with persistent compression, impact with transient compression, distortion, or laceration (Dumont *et al*, 2001a; Sekhon & Fehlings, 2001). The extent of the primary injury often gives a good indication of a patient's prognostic. The first insult to the spinal cord often disrupts only the grey matter (therefore sparing the white matter) and is accompanied by

hemorrhage, disturbing the blood flow inside the entire spinal cord. Neurons that lie within the injury suffer as well from the impact and the hemorrhage and are shown to have a myelin sheath thinner as neurons outside of the lesion (Blight & Young, 1989).

The secondary phase occurs minutes to hours after the primary phase and exhibits inflammation, cell death, ischemia and release of radicals, among other (Ahuja *et al*, 2017) Because some features can be found in both the primary and secondary phases, three stages are describing it more accurately : acute, sub-acute and chronic (Oyinbo, 2011). During the acute phase, sign of ischemia, edema or plasma membrane can be seen (Paterniti *et al*, 2009; Simon *et al*, 2009). These changes happen as well during the sub-acute phase in addition to nitric oxide excess, demyelination of surviving axons or apoptosis (McTigue, 2008; Wu & Ren, 2009). During the chronic phase (that occurs months to years after the injury), the existing demyelination and apoptosis continue and changes in ion channels are seen, as well as syringomyelia and glial scar formation (Schurch *et al*, 1996; Xiong *et al*, 2007).

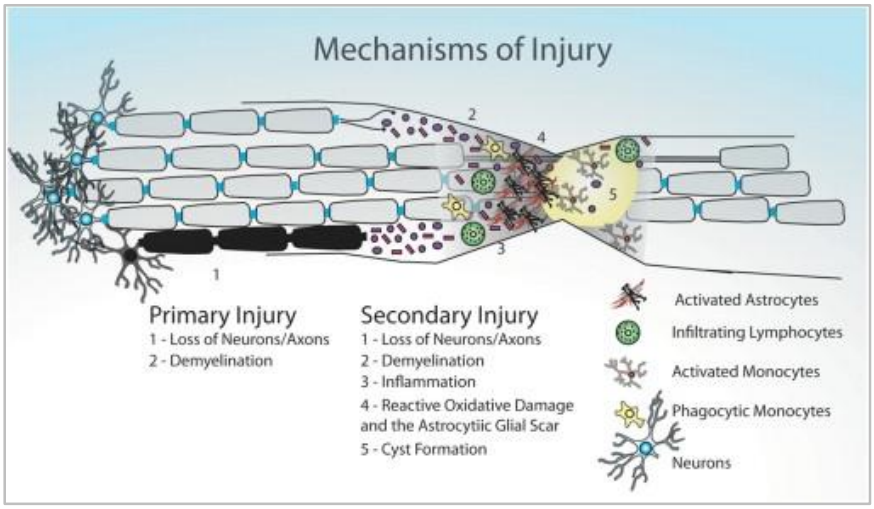

Figure 4 ***Mechanisms of Spinal Cord Injury****: the primary and secondary phase. Reprint permission from (Jorgensen et al, 2015)*

III. Interventions following spinal cord injury

Because SCI is a multi-phase trauma, different approaches can be taken depending on the phase (acute, sub-acute or chronic).

Right after the injury, one of the interventions is done surgically in order to decompress the spinal cord (Fehlings *et al*, 2012; Li *et al*, 2014). Surgical decompression might be beneficial for recovery if performed in the first 24 hours following injury. Because of the impact on the other body's organs, the other course of treatment focuses on the prevention of hypotension and hypoperfusion, both leading to the increase risk of ischemic injury (Dumont *et al*, 2001b). There are as of now, no pharmacological treatments during the acute phase, leading to the targeting of biological mechanisms during the sub-acute and chronic phase. Nevertheless, the use of corticosteroids has been shown to improve the spinal cord oedema during the acute phase. The anti-inflammatory properties of methylprednisolone (MP) make it a good candidate for its administration during the acute phase even if conflicting results were produced (Hall, 1992, 1993). Tirilazad mesylate (TM) was evaluated during the MP trial for its efficacity in the acute phase and showed no improvement but was found to protect against the secondary damages. TM functions as a threefold agent by scavenging lipid peroxyl radicals, preventing lipid peroxidation and stabilizing the membrane, therefore decreasing the membrane fluidity (Hall, 1988), with the difference that, compared to MP, TM does not have some of the steroid side effects, giving a more cerebroprotective efficacity.

Several treatment options were studied and show only partial improvement following SCI, such as opioid receptors antagonists (Bracken & Holford, 1993; Olsson *et al*, 1995), antioxidants and free radical scavengers (Anderson *et al*, 1988; Braughler, 1985) or

calcium/sodium channels blockers (Fehlings *et al*, 1989; Stys *et al*, 1992; Teng & Wrathall, 1997)

During the sub-acute and acute phase, treatments tend to focus on the consequences of the injury. Autonomic dysreflexia (AD) is considered as one of the main emergency following SCI and occurs mostly when the lesion is above thoracic level 6 (Krassioukov *et al*, 2009). Its main characteristics are the elevation of blood pressure, bradycardia, and tachycardia. If not treated, AD can lead to cranial hemorrhage (Eltorai *et al*, 1992; Valles *et al*, 2005), seizures (Yarkony *et al*, 1986) and death (Dolinak & Balraj, 2007). Because AD can be triggered through a common stimulus (irritation to the bladder or colon), efforts are made on preventing it, either surgically or through medication. Botulinum toxin was found to decrease urethral pressure and permitted 6 weeks post treatment to recover continence for 90% of the patients (Dykstra *et al*, 1988; Huang *et al*, 2016; Schurch *et al*, 2000).

Long term care of patients suffering from SCI is as well dealing with depression or pain. Depending on various factors (age, sex, demographic, severity of the injury), depression is shown to affect 1 out of 5 patients and tend to exacerbate lower functional independence and secondary complications (Kalpakjian *et al*, 2009; Khazaeipour *et al*, 2015). Patients benefit from physical exercise, psychological help and when necessary, antidepressants (Fann *et al*, 2015; Fann *et al*, 2013).

Dealing with chronic pain is a challenge for care takers because of the variety and severity of pain (Masri & Keller, 2012; Siddall & Loeser, 2001). Depending on the type of injury (complete or incomplete), patients will suffer differently. An incomplete lesion will lead to muscle spasms, whereas a complete lesion will trigger central dysesthesia syndrome,

more commonly known as phantom pain. This syndrome is the most difficult type of pain to manage because of the wide range of symptoms, sometimes impossible to precisely describe. This pain is poorly understood and badly respond to medication. Multiple clinical trials have been conducted to deal with chronic pain, improving patient's life (Cardenas & Jensen, 2006; Finnerup *et al*, 2002).

During the acute phase, efforts are made to help the patient have some level of recovery below the injury. One main strategy is locomotor training (Behrman & Harkema, 2000; Hubli & Dietz, 2013; Nas *et al*, 2015). Modern strategies do not only try to compensate the disabilities but look at the functional recovery of patients, therefore aiming at neuronal repair and plasticity. Depending on the ASIA score of the patient, different strategies are used. When the injury is below cervical level 8, patients are independent for daily activities, therefore, locomotor training will focus on muscle strengthening, standing and stepping activities. Studies in rats and mice show that treadmill and voluntary training improved motor recovery (Goldshmit *et al*, 2008; Heng & de Leon, 2009; Loy *et al*, 2018). For a patient suffering from quadriplegia, other approaches are taken, as only a few body functions are spared. The use of robotic has become more and more prominent in the past 10 years and show promising results (Edgerton & Roy, 2009; Hornby *et al*, 2005; Louie *et al*, 2015; Yozbatiran *et al*, 2012).

Studies show that following SCI a great decrease in spinal cord, white matter and corticospinal tract volume occur within 2 years post injury (Faden *et al*, 2016; Ziegler *et al*, 2018). These decreases are irreversible and exacerbate the necessity to study and improve SCI outcomes.

IV. Spinal cord injury models

In order to understand SCI mechanisms, researchers developed animal models to mimic the injury and the following biological cascades. Several animals are used, rats primarily (about 72%), followed by mice (16%). Primates and other mammalians, mimicking more closely human SCI, are used in only 7% of the studies because of the relative high costs and ethical consideration (Sharif-Alhoseini *et al*, 2017).

There are three main type of injury model, each one trying to recreate as closely as possible the human SCI.

1. The contusion models

This model is being used in about 43% of the studies and was invented in 1911 by Alfred Allen. He used an impactor where a weight was dropped on an open spinal cord and studied the optimal weight and distance from the cord to recover its functions (Allen, 1911). Since 1911, other contusion apparatuses were invented such as electromagnetic impactors or air gun devices.

The aim of a contusion model is mainly the study of physiopathological changes because during and after SCI, patients suffer from compression and/or contusion (Chang, 2007). The advantage of this technique is the ability to choose the severity of the injury depending on the power of the impact (Figure 5).

Many studies have been conducted using the contusion model to look at the glial scar (Brambilla *et al*, 2005; Iaci *et al*, 2007; Zhang *et al*, 2011), to transplant cells (Martin *et al*, 1996; Tetzlaff *et al*, 2011) or to analyze behavior (Gensel *et al*, 2006; Hamers *et al*, 2001; Ma *et al*, 2001).

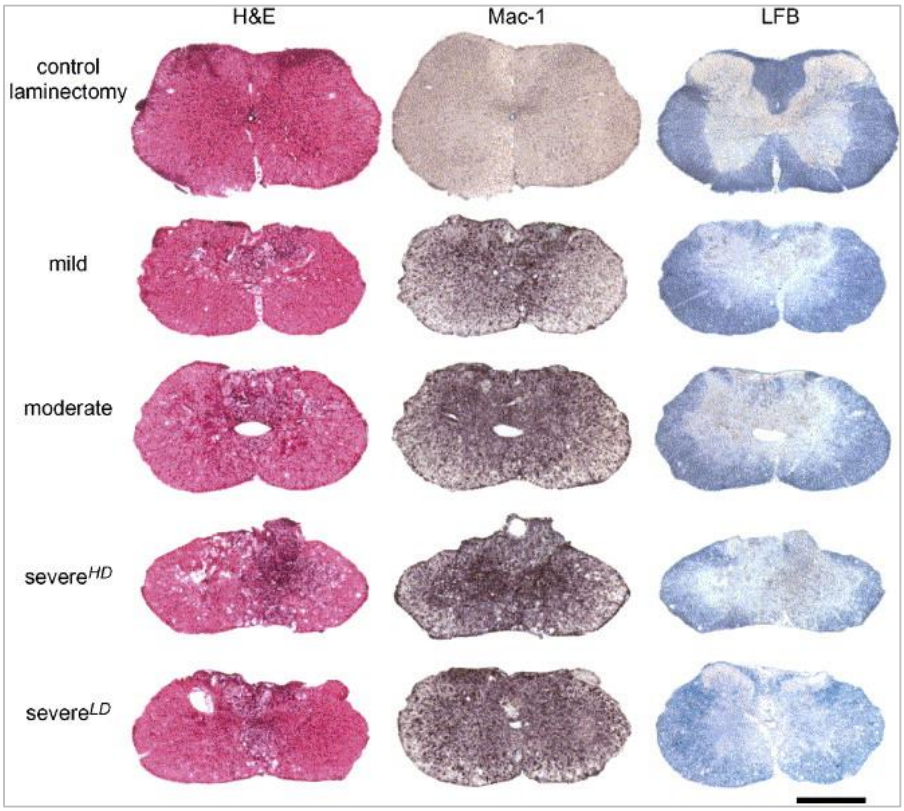

Figure 5 ***Spinal cord cross-sections from laminectomy controls, and the 4 groups of contused mice at the injury epicenter of the lesion, taken 28 days after surgery****. Reprint permission from (Ghasemlou et al., 2005)*

2. The compression models

This model is being used in about 20% of the studies and has the advantage to mimic the human SCI compression and optimal decompression time (Rivlin & Tator, 1978). It enables to cause ischemia and most common clinical injuries. Some apparatus, like the balloon allow to damage the spinal cord in specific area without affecting the surrounding structures (Lim *et al*, 2007; Vanicky *et al*, 2001).

Studies using the compression model look at post injury treatments and decompression time in order to improve post lesion care (Fehlings & Perrin, 2005; Guha *et al*, 1987). They

analyze protein expression as well following injury in order to improve neurological outcome (Curtis *et al*, 1993; Hamada *et al*, 1996; Li *et al*, 1996; Saadoun *et al*, 2008).

3. The transection models

The transection model is the second most used animal model in SCI research. The lesion will be made using iridectomy scissors, allowing a precise and reproducible injury. About 34% of the studies use it and is separated in two groups: complete and incomplete injuries (Figure 6). A complete injury will cut completely the connection between the brain and the lower spinal cord (Courtine *et al*, 2009; Lavrov *et al*, 2006). An incomplete injury will selectively interrupt a specific pathway or tract, allowing the study of specific mechanisms (Bareyre *et al*, 2004; Kim *et al*, 2004; Lavrov *et al.*, 2006; Rosenzweig *et al*, 2010). The interrupted tract can either be a descending/motor tract (Hains *et al*, 2003; Rosenzweig *et al.*, 2010; Sasaki *et al*, 2006), or an ascending/sensory tract (Blesch & Tuszynski, 2003; Inman & Steward, 2003).

Transection models are particularly good to study bioscaffolds, effect of neurotrophic factors on the scar, neuroplasticity or regeneration (Edgerton *et al*, 2004; Gros *et al*, 2010; Liu *et al*, 2012; Schwab & Bartholdi, 1996).

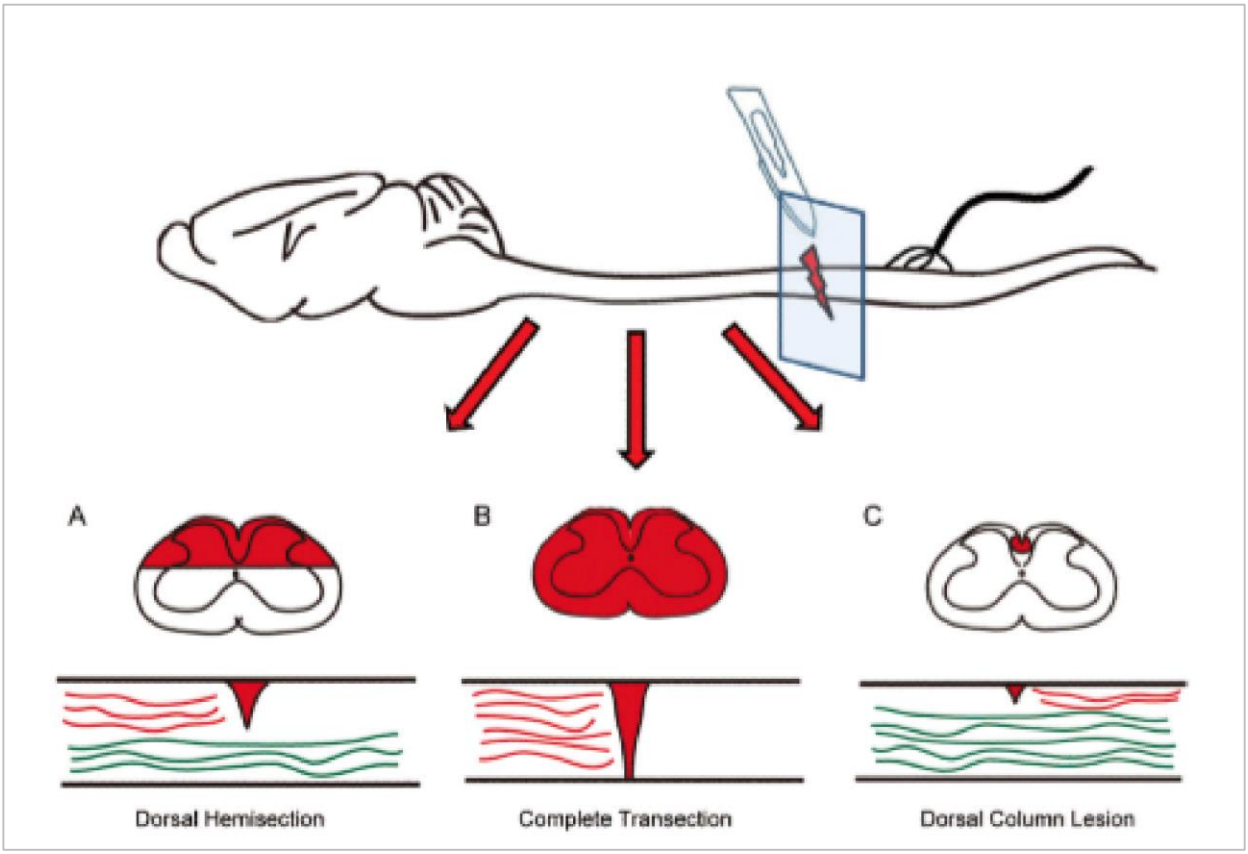

Figure 6 ***Diagram of different mid-thoracic penetrating SCI lesions****. Coronal and sagittal views of the injury site after dorsal hemisection (A), complete transection (B) and a dorsal column lesion (C). After tracers (red) are injected into the cortex (for dorsal hemisection and complete transection) or into the peripheral nerve (for dorsal column lesion), the traced axons typically fail to regenerate across the lesion and are absent from the other side of the spinal cord. Green denotes spared axons that are not labeled by the tracer and intentionally left intact. Reprint permission from Lee, 2013*

V. Remodeling after SCI

1. Spontaneous regeneration

It has been known for decades that cut axons will not regrow through the lesion scar. But after being carefully studied, it was shown that even the adult CNS can remodel, avoiding

the injury site. The first studies corroborating this theory were done in 1981 and used peripheral nerve graft (David & Aguayo, 1981). Two decades were needed to see the same phenomenon in rodent and showed some level of spontaneous recovery as early as four weeks post lesion (Fouad *et al*, 2001). In adults, the same conclusions could be drawn and opened a new therapeutic window for patients with incomplete spinal cord injury (Burns *et al.*, 1997; Curt *et al*, 2004).

Following these findings, research was done looking more closely at ascending and descending tracts that were damaged after the injury. One main example is the corticospinal tract (CST), one of the major descending motor tracts of the spinal cord (Bareyre *et al.*, 2004; Fouad *et al.*, 2001; Lang *et al*, 2012). Other tracts have been studied and show as well spontaneous recovery (Granier *et al.*, 2020; Wang *et al*, 2011).

2. The detour circuit paradigm

Knowing that axons could not regrow through the lesion and scar tissue, one of the main questions of this spontaneous recovery was how axons could reconnect with such distant targets. Fouad et al. first found that the CST could form new collaterals in the cervical region of the spinal cord (Fouad *et al.*, 2001). Bareyre et al. showed that following corticospinal tract lesion, the transected neurons will spread new collaterals in the spinal cord (where there is no lesion) and contact interneurons known as long propriospinal neurons (LPSN). These LPSN will then extend their axons to the lumbar region where they will contact motor neurons therefore creating a detour circuit (Bareyre *et al.*, 2004; Jacobi & Bareyre, 2015) (Figure 7).

This new circuit will allow to reroute the motor input as early as 3 weeks post injury and was shown to be dependent of different factors such as FGF22 and STAT3 (Jacobi *et al*,

2015; Lang *et al*, 2013). It should be noted that motor recovery does not happen alone: without sensory inputs, motor recovery will only be partial. Differing from motor recovery, sensory remodeling hasn't been that extensively studied mostly because of the lack of reliable model but as well due to lack of proper labeling. Hollis et al. showed reorganization of proprioceptive tracts and observed new neuronal connections in the dorsal column allowing some level of recovery (Hollis *et al*, 2015).

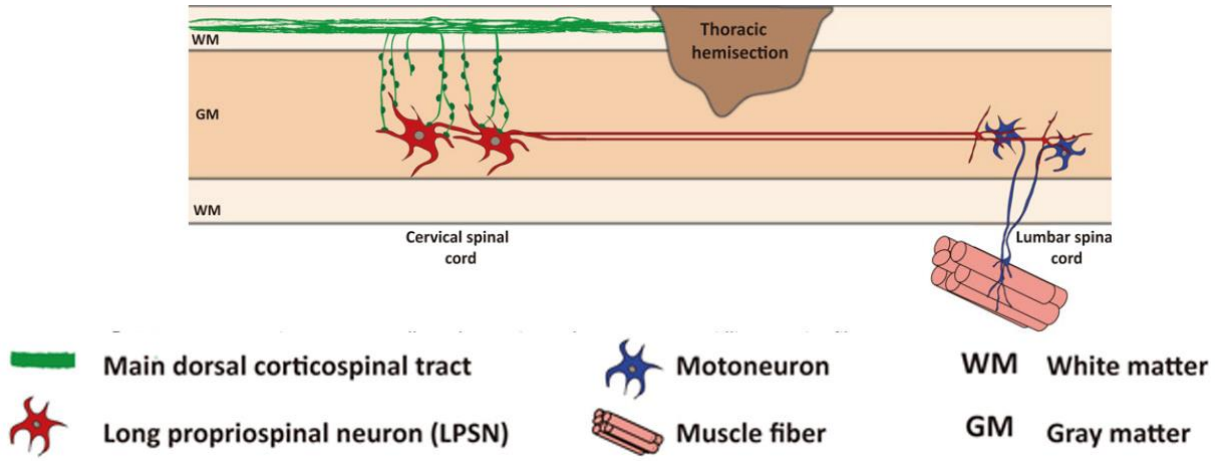

Figure 7 ***Schematic representation of the formation and the regulation of intraspinal detour circuits following spinal cord injury****. Intraspinal detour circuit formation: Following thoracic hemisection, the hindlimb corticospinal tract sprouts collaterals into the cervical spinal cord. Those collaterals form synapses with long propriospinal neurons which in turn increase their contacts onto lumbar motoneurons thereby forming a new detour pathway that reconnects upper corticospinal projection neurons to lumbar motoneurons. Reprint from (Jacobi & Bareyre, 2015)*

3. The somatosensory system

As previously stated, the recovery of the sensory/somatosensory system hasn't been much studied but is necessary for proper motor recovery. To successfully understand this system, one needs to look more into detail how sensory inputs are processed from the spinal cord to the brain.

a. The dorsal column

Also known as dorsal medial lemniscus pathway, this tract is responsible for fine touch, proprioception and vibration sensation from the entire human body. This tract begins in the spinal cord, more specifically in dorsal root ganglions (DRGs), travels in the dorsal column and finishes in one of the nuclei of the brainstem (Figure 8). Fibers ascending from the sacral, lumbar and lower thoracic segment of the spinal cord end in the gracile

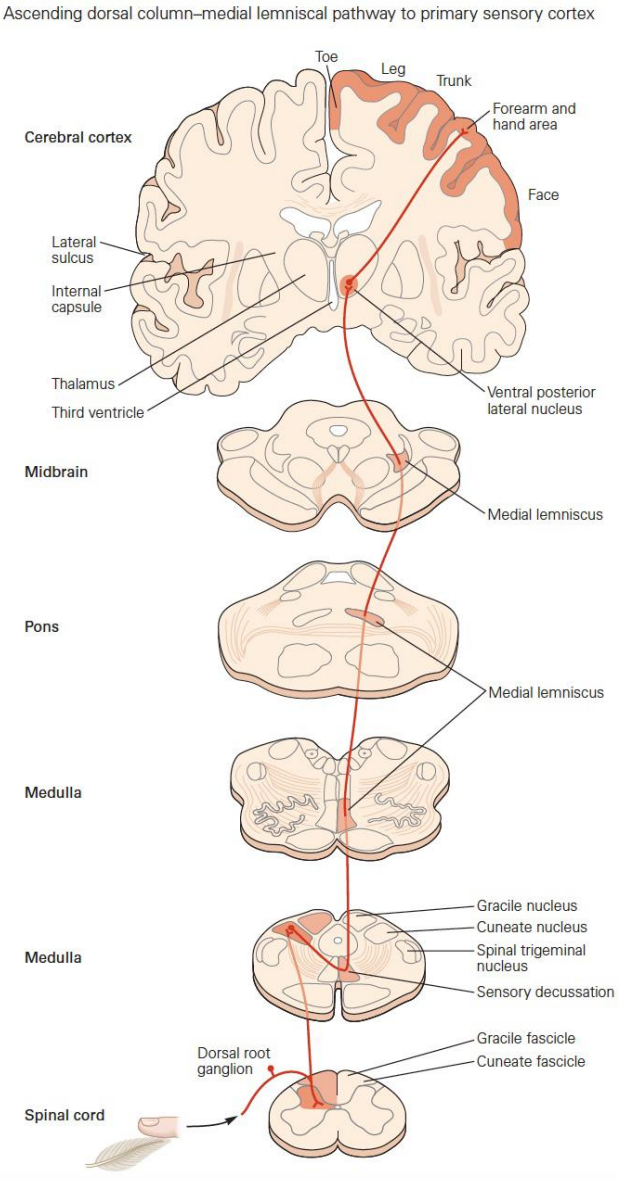

Figure 8 ***Sensory information from the limbs and trunk is conveyed to the thalamus and cerebral cortex by two ascending pathways*** *(Reproduced by Kandel et al., 2013) Copyright © The McGraw-Hill Companies)*

fascicle, fibers from the upper thoracic and cervical in the cuneate fascicle (Kandel *et al*, 2000). This pathway is composed of three orders of neurons: the first order with their cell body in the DRG, project to the medulla oblongata second order neurons (either to the dorsal, gracile or cuneate nucleus). These neurons then project to third order neurons in the thalamus. Inputs arriving in the thalamus are then processed by the primary sensory cortex.

Neurons of the DRG receive their signal from two types of receptors from the skin, mechanoreceptors responsible for tactile inputs and proprioceptive receptors (Al-Chalabi *et al*, 2020). It should be noted that even if both proprioception and tactile axons run in the dorsal column, they remain separated. The proprioceptive run more ventrally whereas the tactile axons run dorsally. Following an incomplete spinal cord injury, it should be known how deep the somatosensory lesion is in order to draw proper conclusions concerning the detour circuit formation.

4. Tracing methods to follow remodeling

Following a dorsal column lesion, the DRG axons will be cut and will not be able to send sensory input to the cuneate nucleus anymore. The connection between DRG and first order neurons will be interrupted. To follow both parts of the circuit, two specific tracers are needed. One anterograde tracer to label DRG neurons and the possible collaterals, one retrograde tracer to label first order neurons and any interneurons projecting to the cuneate nucleus (in the hypothesis of detour circuit formation).

Adeno-associated viruses (AAV) is a viral vector that can be specifically engineered and used in a wide variety of gene therapy. It has unique biophysical and biological properties that make it interesting both in preclinical and clinical research (Naso *et al*, 2017). It has

the ability to deliver inside a host cell different nucleic acid cargo that can be design for one's purpose, labeling neurons, axons and dendrites for example. There are different AAV variants, each being able to infect a specific cell type. An AAV9 will be for example able to cross the blood brain barrier whereas an AAV8 will be more specific for liver delivery (Kattenhorn *et al*, 2016). For the past ten years. AAV have been used as tracers for preclinical research in diverse applications (Cameron *et al*, 2020; Iwakura *et al*, 2005; Smith & Chauhan, 2018). One advantage and disadvantage of AAV is their inability to jump synapses. On one side, it allows tracing of one target and on another side, it restrict their use once interneurons are in play.

In order to label these interneurons, the use of mono-trans-synaptic tracers is necessary.

Rabies viruses travel in neurons retrogradely through multiple synapses. Because of their high efficiency and their ability to jump multiple synapses, new mutants were developed. Mebatsion et al. described a rabies variant lacking the envelope glycoprotein (Mebatsion *et al*, 1996). In this mutant, the glycoprotein gene is replaced by a fluorescent protein, making it a valuable tracer for mono-trans-synaptic labeling. This rabies virus will be able to infect starter cells with high efficiency and can then only infect second degree neurons once complemented with its glycoprotein. Once in the second-degree neurons, the virus will not be able to spread further, being therefore a great tool to label first order connections.

5. Behavioral tests to assess recovery

In the motor system, behavioral testing has been done to look at recovery (Courtine *et al.*, 2009; Goldshmit *et al.*, 2008; Loy *et al.*, 2018). It includes treadmill, where the mouse is place on a running treadmill and captors follow hindlimb movement and the ladder rung,

where the mouse walks on a regular or irregular ladder and counts are being made when it falls (Metz & Whishaw, 2009). Nevertheless, these tests aren't useful in the sensory system. Therefore, proprioceptive, and sensory behavioral tests are required (Shelton *et al.*, 2008). Shelton et al. described experiments that allowed to look at different parameters: proprioception, coordination, or even sensory input (Figure 9)

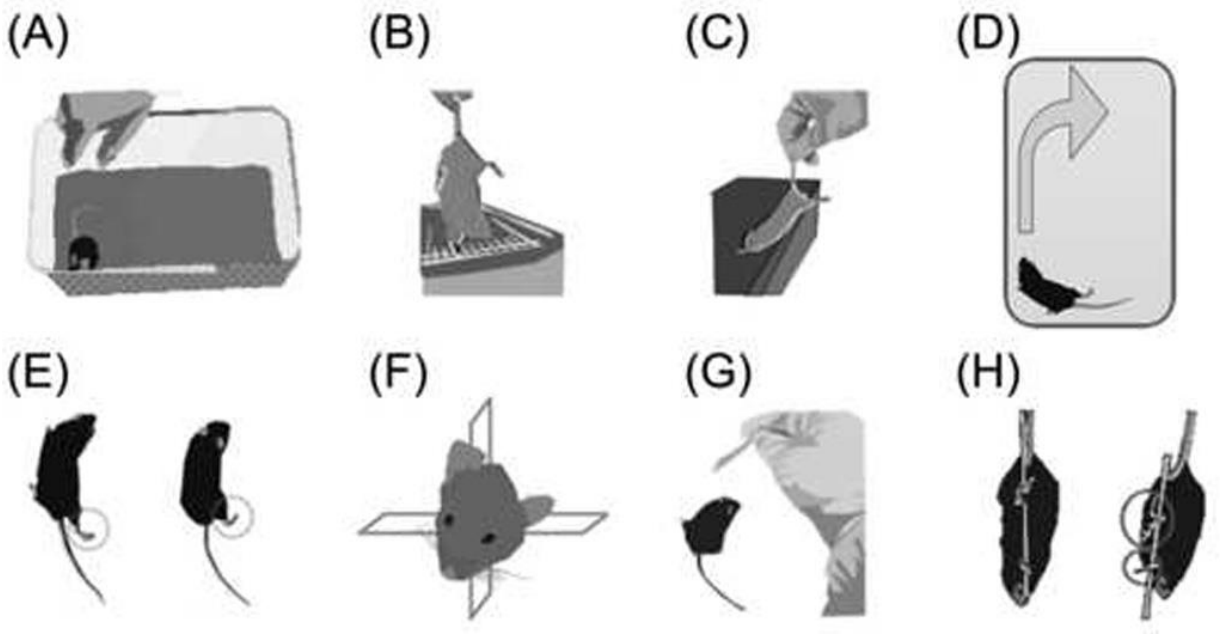

Figure 9 ***Individual SNAP tests.*** *(A) Interactions. (B) Cage grasp. (C) Visual placing. (D) Pacing/circling. (E) Gait/posture. (F) Head tilt. (G) Visual field. (H) Baton. Reprint permission from (Shelton et al, 2008)*

DRG neurons can be divided into three groups depending on their modality: they can be responsible for nociception, mechanoreception or proprioception (Marmigere & Ernfors, 2007). It is as well-known that following spinal cord injury, patients experience phantom pain triggered by nociceptive receptors (Kuffler, 2018). It is therefore important to look as well at pain response following dorsal column lesion. Different tests have been established with the von Frey test being the most popular (Deuis *et al.*, 2017). In this test, the rodent

is placed in a closed cage with a mesh floor, a single filament is perpendicularly applied to the plantar surface of the hind paw and left until the paw buckles (Figure 10A). The response time is then used as readout. Others, such as the tail flick test have been used in smaller settings to decrease the financial cost of such tests.

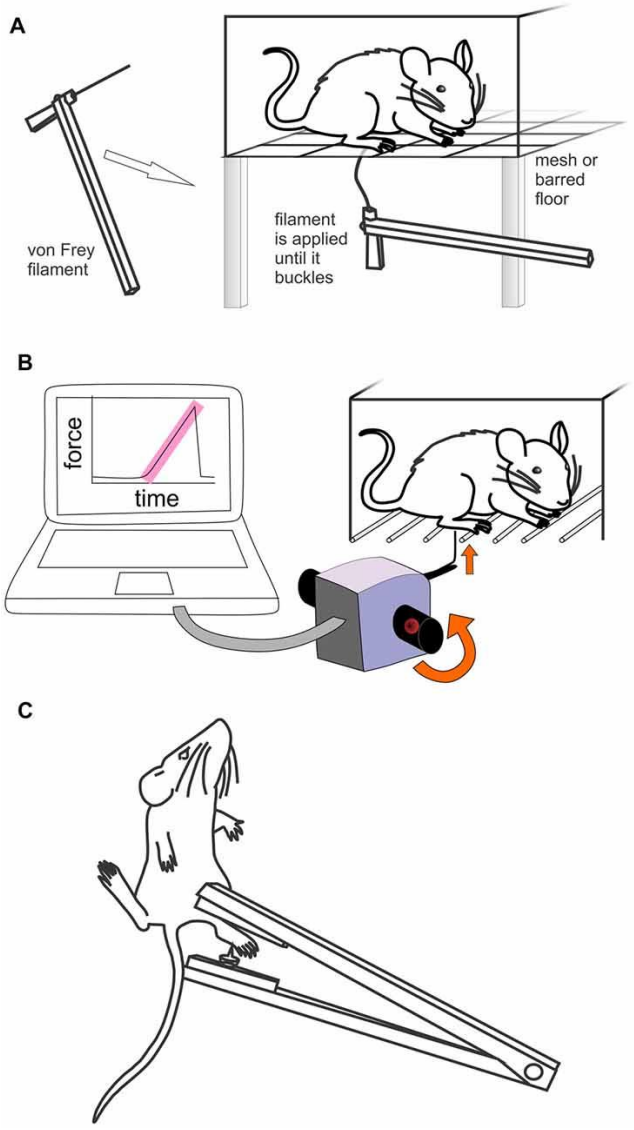

Figure 10 ***Methods used to assess mechanically evoked pain like behaviors in rodents. (A)*** *Manual Von Frey.* ***(B)*** *Electronic von Frey (MouseMet, TopCat Metrology).* ***(C)*** *Randall-Selitto test (handheld device). Open Access (Deuis et al, 2017)*

Chapter 2 Aim of the study

The aim of this thesis was to determine whether plasticity and the formation of detour circuits, like already shown in the motor system, also exist in the sensory system after a dorsal column lesion in mice.

After spinal cord injury are DRG neurons remodeling and is this remodeling targeting specific layers of the spinal cord?

Bareyre et al. (2004) and Jacobi et al. (2015) showed that following spinal cord injury, the CST is able to remodel via LPSN to contact motor neurons in the lumbar region of the spinal cord. It was shown that other tracts remodel following injury. Therefore, the first process to investigate is the change in sprouting of DRG neurons after dorsal column lesion. After lesion, neurons will be traced using an AAV labeled with a EGFP protein and looked at two time points: 3 and 12 weeks. It has been shown that after 3 weeks, the first valuable connections are being made and after 12 weeks, aberrant connections are lost making the mature detour circuit.

a. What are the targets of this new sprouting and what can we learn about them?

In the motor system, LPSN are contacted by CST collaterals to form the detour circuit (Bareyre *et al.*, 2004; Jacobi & Bareyre, 2015). We investigated which neurons were targeted by this increasing DRG sprouting and if the localization of contacts corroborated with the collaterals' varicosities. Characterization of these relay neurons was performed using transgenic mice and immunohistochemistry techniques to assess for the neuronal population primarily targeted by DRG collaterals. After lesion, DRG neurons were labeled using an AAV-EYFP and cuneate nucleus projecting neurons using a pseudotyped rabies

virus complemented with its glycoprotein. Spinal cords were stained for different neurotransmitters, both inhibitory and excitatory.

b. Does formation of a detour circuit in the sensory system triggers functional recovery?

Hollis et al. showed functional recovery following sensory lesion in rats (Hollis *et al.*, 2015) and linked it to remodeling of DRG neurons through the dorsal lemniscal pathway. We investigated behavioral improvement following dorsal column lesion using the forelimb placing and the baton tests (Shelton *et al.*, 2008) as well as the response to a pain test. Mice underwent testing prior to injury and every week after injury up to 12 weeks. Following full recovery, the dorsal column was lesioned again in order to conclude on the implication of the detour circuit formation on functional recovery.

Chapter 3 Materials & Methods

I. Materials

1. Surgery

a. Anesthesia and pain medication

Midazolam-ratiopharm 15mg/3mL	Ratiopharm GmbH, Ulm, Germany
Cepetor® 1mg/mL (Medetomidin)	CP-Pharma Handelsgesellschaft mbH, Burgdorf, Germany
Fentanyl-Janssen 0.1mg	Janssen-Cilag GmbH, Neuss, Germany
Ketamine 10%	Wirtschaftsgenossenschaft deutscher Tierärzte eG, Garbsen, Germany
Xylasin 2% Bernburg	Serunwerk, Bernburg, Germany
Revertor® 5mg/mL (Atipamezol)	CP-Pharma Handelsgesellschaft mbH, Burgdorf, Germany
Flumazenil HEXAL® 0.1mg/mL	Hexal AG, Holzkirchen, Germany
Naloxon-ratiopharm 0.4mg/mL	Ratiopharm GmbH, Ulm, Germany
Metacam	Boehringer Ingelheim International GmbH, Ingelheim, Germany
Temgesic	Merk&Co, Kenilworth, USA

b. Reagents

Panthenol-Augensalbe 5g	Bayer Vital GmbH, Leverkusen, Germany
Xylocain Gel 2%	AstraZeneca GmbH, Wedel, Germany
Isotonische Natriumchlorid 0.9%	Berlin-Chemie Menarini, Berlin, Germany
Ethanol 80%	CLN GmbH Chemikalien Laborbedarf, Niederhummel, Germany

c. Tools and materials

Wella contura	Wella, Darmstadt, Germany

Noyes Spring Scissors	Fine Science Tools GmbH, Heidelberg, Germany
Dumont #5 – Fine Forceps	Fine Science Tools GmbH, Heidelberg, Germany
Dumont #3 Forceps	Fine Science Tools GmbH, Heidelberg, Germany
Olsen-Hegar Needle Holder	Fine Science Tools GmbH, Heidelberg, Germany
Friedman Pearson Rongeur	Fine Science Tools GmbH, Heidelberg, Germany
Vannas Spring Scissors	Fine Science Tools GmbH, Heidelberg, Germany
Plastipak Hypodermic Syringe 1mL	Becton, Dickinson and Company, Franklin Lakes, USA
Sterican Insulin G30 x ½”	B. Braun Melsungen AG, Melsungen, Germany
Hypodermic Needles BD Microlance 3 23G x 1 ¼”	Becton, Dickinson and Company, Franklin Lakes, USA
Metal Plate	Custom-made
Aluminium Short Fixator	Fine Science Tools GmbH, Heidelberg, Germany
Stainless Steel Retractor Wires	Fine Science Tools GmbH, Heidelberg, Germany
Stainless Steel Blunt Retractors	Fine Science Tools GmbH, Heidelberg, Germany
Sugi	Kettenbach GmbH & Co. KG, Eschenburg, Germany
Ethilon Suture 6-0, 667H	Johnson & Johnson Medical GmbH, Norderstedt, Germany
Micropipettes/Capillaries 5µL	Brand GmbH&Co, Wertheim, Germany

d. Devices

Olympus KL 1500 LCD	Olympus Deutschland GmbH, Hamburg, Germany
Olympus Stereo Microscope SZ51	Olympus Deutschland GmbH, Hamburg, Germany
T/Pump Heating pad	Gaymar Industries, Orchard Park (New York), USA
Leica Stereo Microscope M80	Leica Biosystems Nussloch GmbH, Nussloch, Germany
Leica KL 1500 LCD plus	Leica Biosystems Nussloch GmbH, Nussloch, Germany
Vertical Micropipette Puller P-30	Sutter Instrument, Novato, USA

2. Perfusion

a. Devices

IP high precision multichannel pump	Cole-Parmer GmbH, Wertheim, Germany
Digital Scale EK-2000i	A&D, San Jose, USA
Tolloader balance Kern EW (precision scale)	Sigma-Aldrich, Merck KGaA, Darmstadt, Germany
FiveEasy Plus pH/mV (pHmeter)	Mettler-Toledo GmbH, Gießen, Germany
Hotplate Magnetic Stirrer L-82	Labinco BV, Breda, The Netherlands

b. Tools

Pipettes, pipette tips and tubes	Eppendorf AG, Hamburg, Germany
Tubes (15 and 50mL)	Corning, New York, USA
Paper filters	Whatman Schleicher & Schuell GmbH, Dassel, Germany

c. Reagents

PBS 20x (phosphate buffer saline) pH=7.2	5,2 g $NaH_2PO_4 \cdot H_2O$ 28,8g $Na_2HPO_4 \cdot 2H_2O$ 175g NaCl (Merck) 1L dH_2O
Sodium Phosphate Monobasic	27,6 g $NaH_2PO_4xH_2O$
Sodium Phosphate Dibasic	35,6 g $Na_2HPO_4x2H_2O$
0,5M PB (phosphate buffer)	700mL hH_2O 57mL sodium phosphate monobasic 243mL sodium phosphate dibasic
PFA (paraformaldehyde) 4%	40g PFA (Sigma-Aldrich) 500mL 0,2M PB 500µL 1M NaOH

3. Immunohistochemistry

a. Devices

Leica CM1850 Cryostat	Leica Biosystems Nussloch GmbH, Nussloch, Germany
Vortex V-1 plus	Biosan SIA Medical-Biological Research & Technology, Riga, Lettland
Microcentrifuge 3722L	Fisher Scientific GmbH, Schwerte, Germany

b. Tools

Microscope slide	Gerhard Menzel B.V$Co.KG, Braunschweig, Germany
Microscope cover slip 24x32mm	Gerhard Menzel B.V$Co.KG, Braunschweig, Germany
Microscope cover slip 25x50mm	Gerhard Menzel B.V$Co.KG, Braunschweig, Germany
Laboratory Film PM-996	Sigma-Aldrich, Merck KGaA, Darmstadt, Germany
6, 12 and 24-wells cell culture plates	VWR Corporate , Radnor, USA
Tissue-Tek Cryomold® 25x20x5mm	Sakura Finetek Europe B.V., AJ Alphen aan den Rijn, The Netherlands
Tissue-Tek Cryomold® 15x15x5mm	Sakura Finetek Europe B.V., AJ Alphen aan den Rijn, The Netherlands
Tissue-Tek Cryomold® 10x10x5mm	Sakura Finetek Europe B.V., AJ Alphen aan den Rijn, The Netherlands

c. Reagents

Sucrose	Sigma-Aldrich, Merck KGaA, Darmstadt, Germany
Triton X-100	Sigma-Aldrich, Merck KGaA, Darmstadt, Germany
Goat Serum	Invitrogen GmbH, Darmstadt, Germany
Donkey Serum	Invitrogen GmbH, Darmstadt, Germany
Tissue Tek Optimal cutting Temperature	Sakura Finetek Europe B.V., AJ Alphen aan den Rijn, The Netherlands
Vectashield	Vector Laboratories, Burlingame, USA

d. Tracers and antibodies

Rabies virus SAG ΔG mcherry	Provided by Karl-Klaus Conzelmann, Gene Center LMU, Munich
rAAV-CAG-EYFP	Custom made
rAAV-CMV-ECFP-ires-Gprotein	Custom made
Polyclonal rabbit anti-Calcitonin Gene Related Peptide	Sigma-Aldrich, Merck KGaA, Darmstadt, Germany
Monoclonal mouse anti-Parvalbumin	Swant®, Marly, Switzerland
Polyclonal rabbit anti-Glutaminase	Abcam plc, Cambridge, UK
Polyclonal rabbit anti-RFP	Abcam plc, Cambridge, UK
Polyclonal chicken anti-GFP	Abcam plc, Cambridge, UK
Goat anti-rabbit (H+L) Alexa fluor® 488	Abcam plc, Cambridge, UK
Goat anti-rabbit (H+L) Alexa fluor® 594	Invitrogen GmbH, Darmstadt, Germany
Goat anti-rabbit IgG (H+L) Alexa fluor® 647	Invitrogen GmbH, Darmstadt, Germany
Goat anti-mouse IgG (H+L) Alexa fluor®647	Invitrogen GmbH, Darmstadt, Germany
Neurotrace 435/455 blue fluorescent Nissl stain	Invitrogen GmbH, Darmstadt, Germany

4. Counting and Imaging

a. Counting device

Olympus IX71 inverted fluorescence microscope	Olympus GmbH, Hamburg, Germany
Objectives: x4/0.13, x10/0.4 air objectives	Olympus GmbH, Hamburg, Germany

b. Imaging devices

FV1000 confocal system mounted on an upright BX61 microscope	Olympus GmbH, Hamburg, Germany
Objectives: x4/0.13, x10/0.4,x20/0.85 air objectives; x25/1.05 water immersion objective; x40/0.85, x60/1.42 oil immersion objectives	Olympus GmbH, Hamburg, Germany

Leica SP8 Malpighi confocal microscope	Leica Microsystems GmbH, Wetzlar, Germany
Leica DM4 upright microscope	Leica Microsystems GmbH, Wetzlar, Germany
Objectives: x20/1.0 water immersion objective; x40/0.75, x63/1.40 oil immersion objectives	Leica Microsystems GmbH, Wetzlar, Germany

5. Software

a. Data analysis

Microsoft Office (PowerPoint, Excel, Word)	Microsoft Corporation, Redmond, Washington, USA
ImageJ	General Public License http://rsbweb.nih.gov/ij/download.html
Adobe Creative Suite CS6 (Photoshop, Illustrator)	Adobe Systems, Inc., San Jose, California, USA

II. Methods

1. Mice and anesthetics

All animal procedures were performed according to institutional guidelines and were approved by the local regulatory authorities. Mice were maintained on a 12 h light/ 12 h dark cycle with food and water ad libitum.

Adults C57Bl6j, GlyT2-EGFP and GAD67-EGFP (kind gift from Prof. Dr. Arthur Konnerth) mice, 6 to 20 weeks old, were used for this study. To characterize the subtype of the relay neurons, GlyT2 and GAD67 mice, expressing EGFP protein in glycinergic and GABAergic cell, respectively, were used. Unlesioned animals served as controls.

2. Viruses design and production

To generate rAAV-CAG-EYFP, pAAV-CAG-EYFP was created by inserting Enhanced Yellow Fluorescent Protein (EYFP) from pEYFP-N1 into pAAV-CAG-MCS.

pAAV-CAG-ECFP-T2A-G (rAAV-G) was created by inserting ECFP-T2A-G between the EcoRI and HindIII cloning site of pAAV-CAG-MCS. Briefly, ECFP-T2A-G was first PCR-cloned from pAAV-CAG-ECFP onto which the T2A sequence was added using the following forward primer 5' CGCCCA GAATTC ATG GTG AGC AAG GGC GAG GAG CTG TTC 3' and reverse primer 5' CAC GTC ACC GCA TGT TAG AAG ACT TCC TCT GCC CTC TCC GGA TCC CTT GTA CAG CTC GTC CAT GCC GAG AGT 3'. Then, the G envelope protein sequence was PCRed from pCag-GS-CVS-G using as forward primer GAG GGC AGA GGA AGT CTT CTA ACA TGC GGT GAC GTG GAG GAG AAT CCC GGC CCT ATG GTT CCT CAG GTT CTT TTG TTT GTA and as reverse primer GGG CCC AAG CTT CTA GCT TAC AGT CTG ATC TCA CCT CCA. and ligated to the ECFP-T2A fragment. Recombinant AAV chimeric virions containing a 1:1 ratio of AAV1 and AAV2 capsid proteins and the foreign gene were generated as previously described (Grimm & Kay, 2003; Jacobi *et al.*, 2015; Klugmann *et al*, 2005; Lang *et al.*, 2013). Cuneate nucleus projecting neurons were labeled by retrograde monosynaptic tracing with a modified rabies virus (SAD-ΔG-RABV) expression the mcherry fluorescence where mcherry is expressed instead of their own envelope glycoprotein (G). Mono transsynaptic spread to the pre-synaptic partners is only possible when the RABV is complemented with its G-protein.

3. Surgical procedures

a. Cervical dorsal column lesion

Surgeries were performed under constant anesthesia with either a mixture of Ketamine (87 $mg.kg^{-1}$) and Xylasin (13 $mg.kg^{-1}$) or a mixture of Midazolam (5.0 $mg.kg^{-1}$), Medetomidin (0.5 $mg.kg^{-1}$) and Fentanyl (0.05 $mg.kg^{-1}$).

After anesthesia, mice were subjected to a laminectomy in order to expose the dorsal region of the spinal cord at cervical level 2 (C2). A unilateral dorsal hemisection was performed leading to the unilateral transection of the dorsal column, using fine iridectomy scissors and leaving intact all other tracts. Following surgery, an antagonist of MMF composed of a mixture of Atipamezol (2.5 $mg.kg^{-1}$), Flumazenil (0.5 $mg.kg^{-1}$) und Naloxon (1.2 $mg.kg^{-1}$) was subcutaneously injected and an analgesic (Metacam; Boehringer Ingelheim) was orally administered twice a day for 24h. Mice were kept on a heating pad at 38°C until fully awake.

b. Relesion of the dorsal column

Validation of the formation of the detour circuit was assessed using a relesion of the dorsal column 12 weeks after the first C2 lesion. After anesthesia, mice were subjected to a laminectomy in order to expose the dorsal region of the spinal cord at cervical level 4 (C4). A unilateral dorsal hemisection was performed leading to the unilateral transection of the dorsal column, using fine iridectomy scissors and leaving intact all other tracts.

c. Injections of rAAV and SAD-ΔG-RABV

<u>Control, 3 weeks, and 12 weeks remodeling experiments</u>

All viral injections were performed 10 days prior to sacrifice. To label DRG axons we pressure injected 0.5µL of rAAV-EYFP (concentration of 5.10^{11} genome copies/mL) into the DRG at cervical level 6 (C6) using a finely pulled glass micropipette (coordinate from DRG surface 0.3mm depth). To visualize the injection, a blue dye was added to the rAAV. The micropipette was left in place for three minutes following the injection to avoid backflow. To label cuneate nucleus projecting neurons, a 1:1 mixture of SAD-ΔG-RABV and rAAV-CAG-G (concentration matched to 5.10^{5} and $1,5.10^{10}$ genome copies/mL respectively) was injected into the cuneate nucleus. In brief, the mouse was place on its back and held in place, a fine incision (10 mm long) was done under the jar to access the medulla oblongata ventrally, holding the trachea on the side using retractors. Once the medulla oblongata was exposed, the central vessel was used as a zero. Then, 0.25µL RABV and rAAV mixture was pressure-injected using a finely pulled glass micropipette (coordinate from central vessel: 0.2 mm, 0.9 lateral, 2.0 depth). After completing the injection, the micropipette was left in place for five minutes. Following surgery an analgesic (Metacam; Boehringer Ingelheim) was orally administered twice a day for 24h, 1000 µl 0,9% Saline solution (B.Braun Melsungen AG) was subcutaneously injected as rehydration and the mice were kept on a heating pad at 38°C until fully awake.

4. Tissue processing and immunohistochemistry

Mice were deeply anesthetized using isoflurane and perfused transcardially with 4% paraformaldehyde (PFA) in 0.1M phosphate buffer (Hornby *et al.*). Brains, spinal cord and injected DRG were then microdissected and post fixed overnight in 4% PFA. The tissue was cryoprotected in 30% sucrose up to 48h. Using a cryostat, 50 µm thickness sections

were cut (longitudinal sections for basic neuroanatomy of the ascending DRG system and the DRG sprouting, coronal sections for all other analysis). For the analysis of the tract organization, the DRG sprouting, the DRG axons localization, the cuneate nucleus projecting neurons localization, the number of contacted neurons and number of contacts onto single neurons, a counterstaining was performed with NeuroTrace 435/455 and sections were mounted in Vectashield (Vector Laboratories).

To visualize CGRP and PV expressing neurons, immunohistochemical staining was performed on C57/Bl6, GlyT2 and GAD67 mice, as follows: Half of the wells and slides per animal were used for the histological analysis, while the rest were kept at 4°C for wells with 0.01% PBS-azide and -20°C for slides. The first day sections were washed three times in Phosphate-buffered saline (1xPBS) of ten minutes intervals and incubated for 1h in a blocking PBS-based solution with 0.5% Triton X-100 and 10% goat-serum (GS). Slices were then incubated at 4°C in a PBS-based solution containing primary antibody against CGRP or PV, 0.3% Triton X-100 and 2.5% GS, for two overnights. The third day and after three ten-minutes intervals washing in 1xPBS, sections were incubated overnight at 4°C with the respective secondary antibody (AF647) and NeuroTrace 435/455 diluted in 1XPBS with 1% GS. Finally, tissue was washed three times at 15 to 20 minutes intervals to minimize background noise, mounted with Vectashield (Vector Laboratories) and stored at -20°C. To visualize glutamatergic neurons antigen retrieval was performed prior to the staining. Because antigen retrieval diminishes all signal including the yellow and red fluorescence from the injected EYFP and mCherry viruses, antibodies against GFP and RFP were used, allowing this method to be performed only on C57/Bl6 mice lacking transgenic GFP signal. Heat-mediated antigen retrieval was carried out as described: Citrate buffer was prepared by adding and mixing 2,94g of Tri-

Sodium citrate (Sigma) with 1L distilled water for a final concentration of 10mM. pH was adjusted to 8.5 by adding drops of 1M HCl or 1M NAOH.

Appropriate amount of citrate buffer, according to the number of wells, was heated to 85°C and 500ul were distributed immediately in each well. The well plate was carefully sealed, top and sides, with 3 layers of parafilm. Tissue was incubated with the heated buffer in a water bath set at 85°C, for 30 minutes. Parafilm and lid were then removed, and the plate was left to cool at room temperature for 10 minutes. Sections were then washed three times of ten minutes' intervals in 1x PBS. Hereafter, sections were incubated in blocking PBS-based buffer containing 0.5% Triton X-100 and 5% GS. Blocking buffer was replaced with the 1xPBS based solution including 0.3% Triton X- 100, 2.5% GS and the primary antibodies, anti-glutaminase and anti-GFP, and tissue was incubated at 4°C overnight. The second day, slices were washed three times for ten minutes in 1XPBS and were incubated overnight with the respective secondary antibodies diluted in 1xPBS solution with 1% GS.

After washing at fifteen-minutes intervals, slices were incubated with primary antibody against RFP, in 1XPBS buffer with 0.3% Triton X-100 and 2.5% GS, overnight. Secondary antibody, AF594, along with the NT-435/455, diluted in 1xPBS buffer containing 1% GS, was applied after washing and left overnight for incubation. Finally, slices were washed three times with a minimum of fifteen minutes' intervals. Tissue was mounted on slides and coverslipped using Vectashield mounting medium (Vector Laboratories) and stored at -20°C.

In order to characterize as many cuneate nucleus projecting neurons as possible, the already stained and scanned slides from control, 3-weeks, and 12-weeks after injury

GlyT2 and GAD67 groups underwent a second histological analysis. Slides were unmounted carefully and placed in well plates. Heat-mediated antigen retrieval was performed as described above in order to remove all existing fluorescent signal and re-stain for glutaminase. Following the antigen-retrieval, sections were washed three times of ten minutes' intervals in 1x PBS and were incubated in blocking PBS- based buffer containing 0.5% Triton X-100 and 5% GS. Slices were then incubated overnight with the primary antibody for glutaminase in a 1xPBS based solution including 0.3% Triton X-100 and 2.5% GS. The second day, slices were washed in 1XPBS and were incubated overnight with the respective secondary antibody AF488 diluted in 1xPBS solution with 1% GS. Finally, slices were washed three times with minimum fifteen minutes' intervals. Tissue was mounted on slides using Vectashield as mounting medium and stored at -20°C.

5. Imaging

All images were acquired using automated confocal scanning of spinal cord tissue with the FV10-ASW microscopy software on an upright Olympus FV1000 confocal microscope system. Images were obtained using standard filter sets and acquisition settings were kept constant between control and post-injury groups for each experiment. To assess the density of spinal DRG collaterals four sections per animals were randomly chosen and for each section, four frames were scanned at 20 × magnification (objective: Olympus UPLSAPO 20XO, imaging medium: Olympus IMMOIL-F30CC, NA: 0.85; 640 × 640 pixels, zoom × 1.1, 0.45 µm z-resolution, 16bit). Image fields of view were positioned so that their medial borders aligned with the top of the spinal cord. At this magnification, all of white and gray matter was included, allowing the detection of all spinal DRG collaterals.

As described earlier, DRG axons were labeled with EYFP (AAV-EYFP), and cuneate nucleus-projecting neurons were labeled with RABV-mCherry. Images were acquired as stacks (tile scan acquisition) from 50µm thickness sections, using upright Leica SP8 WLL confocal microscope. 3 sections per antibody, per animal randomly chosen between C4 and C6 cervical level were imaged. Sections were scanned at their right-half side, where the DRG sprouting axons were injected with the rAAV-CAG-EYFP. Image acquisition settings on the confocal were as follows: (i) scanning conducted in a sequential mode between frames with a x20/0.75 NA oil-immersion objective, (ii) resolution 2.048x2.048, (iii) frame average 4, (iv) step-size set to 1.5um and (v) zoom at 0.75. Any laser line could be generated by the microscope's laser and the fluorescent signals were scanned in pairs using the Hybrid-Detectors (HyD). NeuroTrace 435/455 and mCherry were scanned together, EGFP with far-red (pseudocolored magenta) and EYFP alone. To avoid any overlap between the fluorescent signals the excitation and detection wavelengths were carefully set individually for each section, depending on the intensity of the signal. C57/Bl6 mice images acquired with the same settings, but the fluorescent signals were different. GFP with AF488 was used for visualization of DRG sprouting axons as we have no transgene signal and RFP with AF 594 for cuneate nucleus projecting neurons. As a result, AF488 –sprouting collaterals- and AF647 -used for CGRP, PV or glutaminase staining- were scanned separately and NeuroTrace 435/455 was scanned simultaneously with AF594. Tiles were automatically stitched by the Leica Software.

6. Image processing

Images obtained with confocal microscopy (Leica SP8 and Olympus FV1000) and fluorescence microscope (DM4) were processed using ImageJ software to generate

maximum intensity projections. In order to obtain final images, the maximum intensity projections were processed in Adobe Photoshop using levels and gamma adjustments to enhance visibility of intermediate grey values. For visualizing the co-localization of cuneate nucleus projecting neurons and all staining/transgenic expression, both signals were pseudocolored before being overlaid using ImageJ software.

7. Quantification

a. Quantification of DRG sprouting

To evaluate the sprouting of DRG axons, longitudinal sections of the spinal cord (50 µm thickness) were acquired with an Olympus FV1000 confocal microscope equipped with standard filter sets and a x20/0.85 objective. The number of collaterals was counted. The total number of DRG axons was calculated using the tubeness tool of ImageJ software averaging on three coronal sections for each spinal cord at cervical level 7. The number of collaterals per axon was then calculated. All quantifications were performed by an observer blinded with respect to injury status and time point.

b. Quantification of the DRG axons localization

To evaluate the localization of DRG axons following a sensory lesion, 15 coronal sections spanning the C3 to C6 area of the cervical spinal cord (50 µm thickness, every fifth section) were analyzed under a fluorescence microscope (Olympus IX71) with a x40/0.65 air objective. The boutons were categorized as dorsal, intermediate, or ventral depending on their localization in the spinal cord (in layer I to IV: dorsal, V to VII: Intermediate and VIII to IX: ventral respectively). A bouton was defined as a thick varicosity along a comparably thin DRG axon in the cervical spinal cord. The number of boutons was expressed as percentage of all DRG axons boutons evaluated in the cervical spinal cord.

All quantifications were performed by an observer blinded with respect to injury status and time point.

c. Quantification of the localization of cuneate nucleus projecting neurons

To evaluate the localization of relay neurons following dorsal column lesion, every coronal section containing a cuneate nucleus labelled neuron (with the RABV) spanning the C3 to C6 area of the cervical spinal cord (50 µm thickness) were analyzed under a fluorescence microscope (Olympus IX71) with a x10/0.25 air objective. The neurons were categorized as dorsal, intermediate, or ventral depending on their localization in the spinal cord (in layer I to IV: dorsal, V to VII: intermediate and VIII to IX: ventral respectively). The number of neurons was expressed as percentage of all cuneate nucleus projecting neurons evaluated in the cervical spinal cord. All quantifications were performed by an observer blinded with respect to injury status and time point.

d. Quantification of the number of contacted neurons and the number of contacts onto single neuron

To evaluate the number of contacted neurons and the number of contacts onto single neurons, every coronal section containing a cuneate nucleus labelled neurons (with RABV) spanning the C3 to C6 area of the cervical spinal cord (50 µm thickness) were acquired with an Olympus FV1000 confocal microscope equipped with standard filter sets and a x20/0.85 oil immersion objective (zoom 1.5, step size 0.5 µm). All single planes from the image stacks were analyzed in order to assess the presence of a bouton (as described above) on a cuneate nucleus projecting neuron (dendrite/axon or cell body). Both values were normalized according to the number of labelled DRG fibers and cuneate nucleus projecting neurons. Briefly, the total number of DRG axons was calculated using the

tubeness tool of ImageJ software averaging on three coronal sections for each spinal cord at cervical level 7. The number of cuneate nucleus projecting neurons was normalized for efficiency by averaging the number of labelled neurons (with the RABV) in three coronal sections rostral to the lesion level (C2). The number of contacted neurons was expressed as percentage of the total number of cuneate nucleus projecting neurons between C3 and C6 of the spinal cord. The number of contacts onto single neuron was obtained by dividing the total number of contacts by the total number of contacted neurons. All quantifications were performed by an observer blinded with respect to injury status and time point.

e. Quantification of the interneurons localization and subtype

For all labelled neurons (mCherry, pseudocolored red, cuneate nucleus projecting neurons, transgenic GFP-positive, pseudocolored green, glycinergic or GABAergic neurons and far-red, pseudocolored magenta, CGRP or PV expressing neurons) except the glutamatergic ones, quantification was done on maximum intensity projections. Image stacks were first loaded on ImageJ and z-project/maximum intensity projection was generated. Using Adobe Photoshop and based on the Allen Brain Atlas- Mouse Spinal Cord Reference Atlas, the spinal cord was divided into dorsal (laminae I-IV), intermediate (laminae V-VII, X) and ventral (laminae VIII-IX) areas. The number of each interneuron subtype was counted for each area using the cell counter tool of ImageJ and all areas' numbers for each subtype were added to give the sum. The number of single-, double- or triple-positive cuneate nucleus projecting neurons was counted separately in each spinal cord area. The total number was then calculated. Because of the high noise-to signal ratio for the glutaminase staining, it was very inaccurate to count the cell number on maximum intensity projections. For this purpose, in glutaminase stained sections counting was done

directly on the Image stacks and maximum projections were only used to separate the laminae into areas and for pointing the cells' numbers using again the cell counter tool provided by ImageJ.

In order to quantify the number of contacts onto interneurons all single planes from the image stacks were analyzed. A contact was defined as the presence of a bouton, a thick varicosity (about three time the diameter of a relatively thick DRG axon) (EYFP positive and pseudocolored yellow) closely apposed to an interneuron's soma, dendrite, or axon. To facilitate counting for each subtype in each area (dorsal, intermediate, ventral) cell counter tool of ImageJ was used to point the contacts on the maximum intensity projections. Contacts for each subtype and area were given a different number. Moreover, contacts on single-, double- and triple-positive cuneate nucleus projecting neurons were separately counted using again different numbers for each area. For each category, numbers were summed to obtain the total number of contacts per condition for each section.

8. Behavioral analysis

The following behavioral tests were used to assess recovery after spinal cord injury (Deuis *et al.*, 2017; Shelton *et al.*, 2008)

a. Forelimb placing response

To assess proprioception, the visual placing test was used. In brief, the mouse is held suspended by the tail next to a table edge. The mouse is slowly advanced toward the edge of the table with its torso. A mouse without injury would extend its upper torso and paws simultaneously to reach the edge of the table. Prior to baseline, all mice underwent

three familiarization sessions. Following familiarization, each mouse is recorded and allowed to reach the edge three times. Each trial is then scored from 0 to 4 with (0) once aware of the edge, arches back and reaches out with both forepaws, (1) reach with both paws but uninjured paw leads, (2) does not reach occasionally with injured paw, (3) does not reach at all with injured paw, (4) head does not raise and does not reach with both paws. For each mouse, an average of the three score is calculated.

b. "Baton"

As a second proprioceptive test, the baton test was conducted. Briefly, the mouse is held suspended by the tail and allowed to grasp a 5-mm diameter stick with its forelimbs. After the mouse grasps the applicator, it is released while the mouse remains suspended. A mouse without injury would grasp the applicator with both forelimbs. Prior to baseline, all mice underwent three familiarization sessions. Following familiarization, each mouse is recorded and allowed to grasp the applicator three times. Each trial is then graded from 0 to 4 with (0) grasp with both forelimbs, (1) grasp with both forelimbs but loses grasp with injured paw, (2) does not grasp occasionally with injured paw, (3) does not grasp frequently with injured paw, (4) does not grasp with injured paw at all. For each mouse, an average of the three score is calculated.

c. The tail flick test

As nociception test, the tail flick test was conducted. Briefly, the mouse is held in a tube closed on one end. Its tail is held without pressure between two fingers and immersed in a water bath at 50 degrees Celsius. The test is ended once the tail flicks. Prior to baseline no familiarization session is performed to prevent adaptative responses. Each mouse is recorded, and the tail immersed three times. Evaluation of the flick time is then

processed using the recorded videos. For each mouse, the average of the three times is calculated.

9. Statistical evaluation

All results are given as mean ± SEM. GraphPad Prism 7 for Windows (GraphPad software) was used to perform the statistical analysis. To compare two groups, student's t-tests were used. In case of multiple comparison, a one-way ANOVA followed by a Tuckey *post hoc* test was performed. Significance levels are indicated as follow: * or # $p<0.05$; ** or ## $p<0.01$; *** or ### $p<0.001$.

Chapter 4 Results

Each experiment of this chapter was performed following the same timeline, and mice were divided into three groups: control or unlesioned mice, 3 weeks, and 12 weeks timepoints. A unilateral dorsal column lesion was performed at level C2, one DRG at level C6 was labeled using an AAV expressing EGFP or EYFP (Figure 11a) and a pseudotyped rabies virus and complementary glycoprotein were injected in the cuneate nucleus in the medulla oblongata (Figure 11b). Tracers were always injected 10 days prior to sacrifice and following dissection, spinal cord were either cut longitudinally (to see the dorsal column from C2 to C6 regions) or coronally (to see the DRG sprouting in the gray matter)

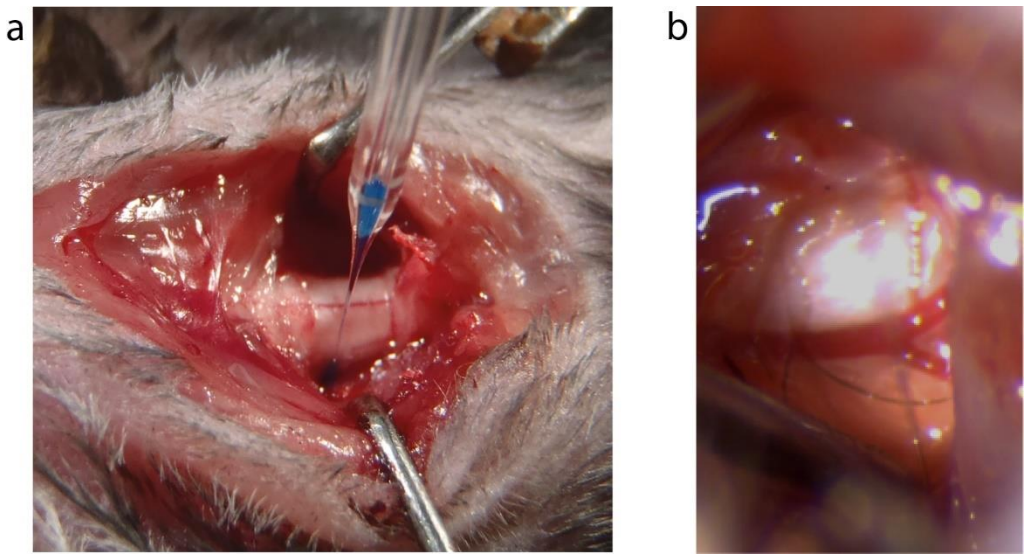

Figure 11 ***Labeling of DRG cuneate nucleus neurons in mice.*** *Picture of (a) a AAV-EYFP injection in an exposed spinal cord DRG at level C6 and (b) a mcherry rabies virus from a ventral approach.*

I. DRG neurons send new collaterals in the spinal cord

Work from MD thesis from Julian Schwarting and Fabian Laage-Gaupp.

For this experiment, mice were only labeled using the AAV-EGFP (Figure 12a). We could observe that even in an unlesioned animal, DRG axons send collaterals in the grey matter of the spinal cord (Figure 12b top). Nevertheless, following dorsal column lesion, DRG axons sprouts significantly already 3 weeks post injury (Figure 12b middle). After 12 weeks, we noticed that this sprouting was reduced but still significantly increased compared to control (Figure 12b bottom). When quantified a 90% and 55% increase was observed 3- and 12-weeks post injury, respectively (Figure 12c).

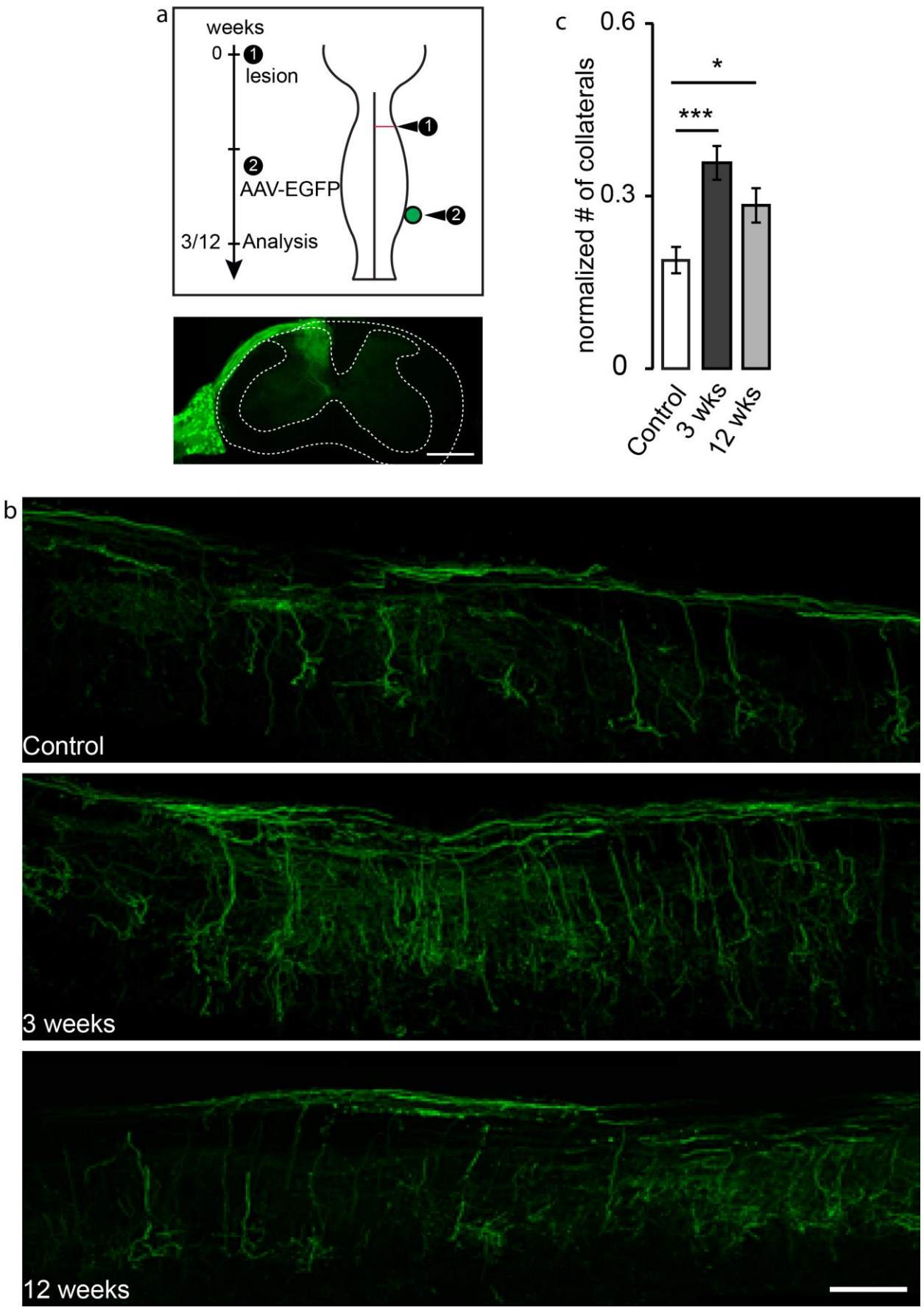
a
weeks
0
1
lesion
2
AAV-EGFP
3/12
Analysis
c
normalized # of collaterals
0.6
0.3
0
*
***
Control
3 wks
12 wks
b
Control
3 weeks
12 weeks

Figure 12 ***DRG neurons send new collaterals in the spinal cord****. (a) Timeline, lesion and injection site of the experiment and confocal picture of a DRG labeled using an AAV-EGFP (b) Confocal images of cervical DRG collaterals exiting into the grey matter in mice at 3 and 12 weeks post injury as well as control (c) Quantification of the number of collaterals exiting into the cervical grey matter (***: p<0.0001; *:p<0.01 n=10-17 mice per group) from (Granier et al., 2020)*

It was then questioned if this sprouting might target different areas of the spinal cord (dorsal, intermediate, or ventral layers). Therefore, the spinal cord sections labeled with AAV-EGFP were cut coronally, the number of varicosities were counted and a total number as well as a percentage of total varicosities was assessed (Figure 13a).

It was first noticed that following injury, the total number of varicosities increased (Figure 13b and c). We could see as well that in control mice, these varicosities were mostly in the intermediate and dorsal part of the spinal cord. But following injury a shift in dorsal sprouting was observed (Figure 13d).

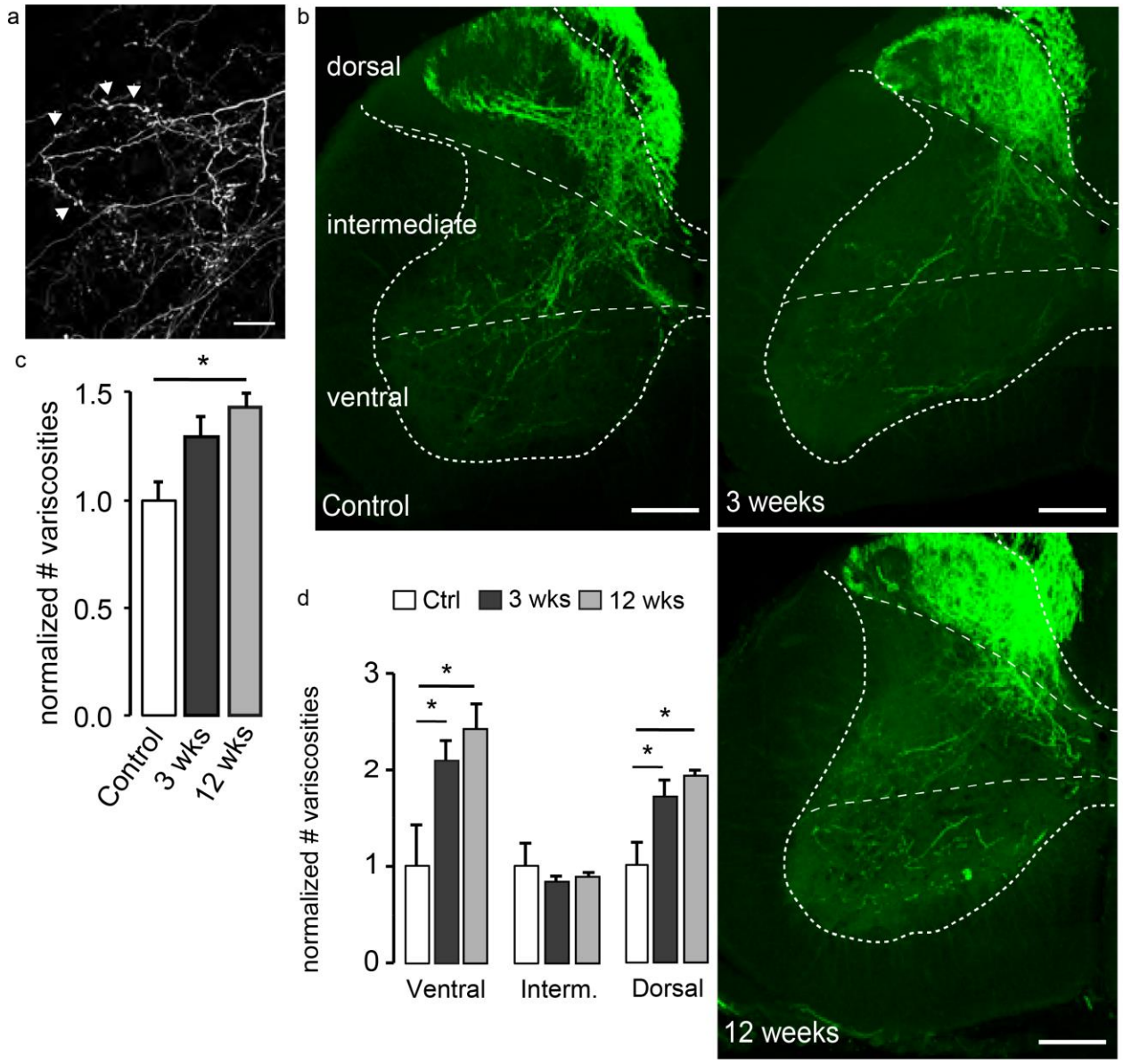

Figure 13 ***DRG sprouting target different area of the spinal cord following injury.*** *(a) Representative confocal image of the varicosities quantified on DRG axon collaterals (control animal). (b) Coronal confocal image of cervical DRG collaterals exiting into the grey matter in unlesioned (control) and lesioned mice at 3 and 12 post injury. Lines on the spinal cord represent the different areas analyzed (dorsal/intermediate and ventral). (c) Quantification of the normalized number of varicosities and their change following the lesion. (d) Localization of DRG varicosities in the ventral, intermediate and dorsal parts of the cervical spinal cord. Medial: *p<0.01. From (Granier et al, 2020)*

These findings indicated that because of the injury, DRG axons sent new sprouting in the spinal cord to target new or existing neurons and therefore form a new circuit.

Nevertheless, nothing is yet known about these new targets and if these varicosities are functional. To answer this question, some staining revealing either Basoon or Synapsin could be done.

II. DRG neurons send collaterals in the spinal cord to contact cuneate nucleus neurons.

For this experiment, mice were both labeled using the AAV-EYFP in the DRG at level C6 and the mcherry rabies virus (Figure 14a). As it is known that DRG neurons project to the cuneate nucleus through the dorsal column lemniscal pathway, we thought that any contact made by these new DRG collaterals might be onto cuneate nucleus projecting neurons. In order to be sure of the specificity of the injection in the cuneate nucleus, control mice were injected with the rabies virus and its complementary glycoprotein. As it allows to see first order connection, the fluorescence will travel from the cuneate nucleus neurons to its pre-synaptic partner in the DRG. Therefore, successful injection will be noticeable through mcherry fluorescence in the DRG (Figure14b, arrow).

First, the localization of these cuneate nucleus projecting neurons was assessed. We saw that in a control mouse, these neurons were mostly in the dorsal and intermediate layers of the spinal cord. Following lesion, already 3 weeks but even more 12 weeks post injury, most of the cuneate projecting neurons were localized in the intermediate layers (Figure 14c).

Through the double labeling, we were able to confirm contact formation between DRG axons and cuneate nucleus neurons, therefore validating the detour circuit hypothesis.

Moreover, we could see that about 20% of all cuneate nucleus projecting neurons were contacted in a control situation. Three weeks following injury, this number increase significantly to 40% to decrease 12 weeks post injury (Figure 14d). We looked as well at the location of these contacted cuneate nucleus neurons and could confirm our previous results that they were mostly located in the intermediate and dorsal layers of the spinal cord (Figure 14e). Additionally, not only the total number of contacted cuneate neurons increased but as well the number of contacts per cuneate nucleus neuron (Figure 14f). To obtain this information, single plain analysis was performed: every coronal section containing a cuneate nucleus labelled neuron spanning the C3 to C6 area of the cervical spinal cord was acquired with a confocal microscope (step size 0.5 µm) and all single planes from the image stacks were analyzed (Figure 14g). We saw that even if the total number or cuneate nucleus neurons got reduced 12 weeks post injury, each neuron was significantly more contacted by DRG collaterals (Figure 14h). This could mean that the refinement happening between 3- and 12-weeks post lesion strengthened the valuable new connections, allowing the detour circuit to convey functional recovery.

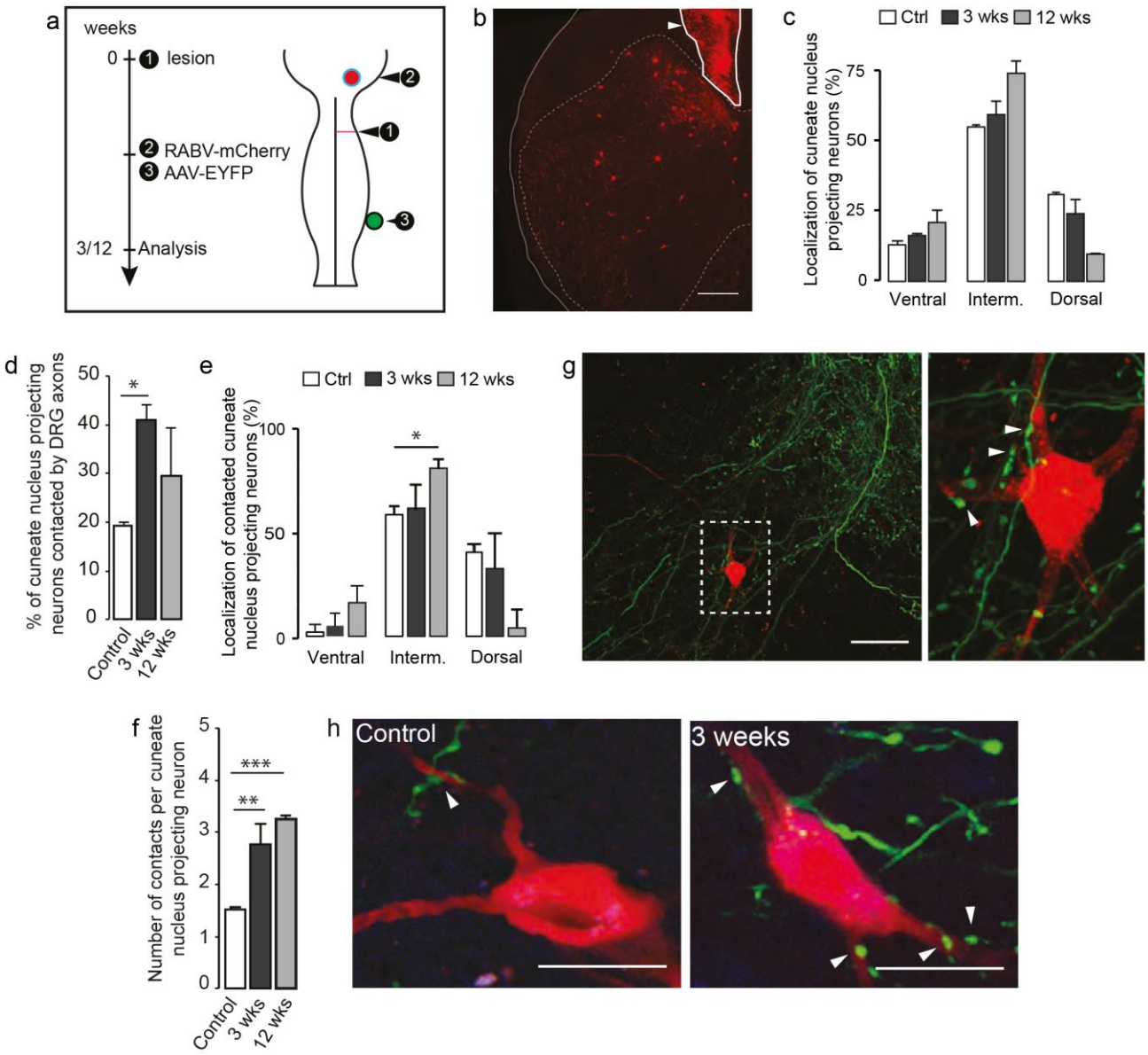

Figure 14 ***DRG collaterals target cuneate nucleus projecting neurons****. (a) Timeline, lesion and injection site of the experiment (b) Confocal picture of a spinal cord section labeled with an mcherry rabies virus (control mouse). (c) Quantification of the localization of cuneate nucleus projecting neurons in unlesioned (control) and lesioned mice at 3- and 12-weeks post injury. (d) Quantification of the localization of contacted cuneate nucleus projecting neurons in unlesioned (control) and lesioned mice at 3- and 12-weeks post injury. (* p<0.01 control vs 3 weeks (e) Quantifications of the localization of contacted cuneate nucleus projecting neurons in unlesioned (control) and lesioned mice at 3- and 12-weeks post injury. (* p<0.01 control vs 12 weeks) (f) Quantifications of the number of contacts per cuneate nucleus neuron (** p<0.001 control vs 3weeks and *** p<0,0001 control vs 12 weeks) (g) Representative confocal images of appositions between cuneate nucleus projecting neurons and DRG collaterals in the cervical spinal cord (arrows point to appositions) (h) Representative confocal images of appositions between relay neurons and DRG collaterals. Quantification of the total number of contacts per timepoints. Data analyzed using 2-way ANOVA followed by Dunnett's multiple comparisons test. Scale bars equal 300µm in (b), 50 µm in (g); right panel is a 3-times magnification of the boxed area) and 15 µm in (h). from (Granier et al., 2020)*

In the event that these connections were functional synapses, the relay of sensory input could potentially be restored.

III. New connections between DRG and cuneate nucleus allow proprioceptive recovery.

To assess proprioceptive recovery two tests were performed: the forelimb placing response and the baton test (Shelton *et al.*, 2008). The forelimb placing response is done with the mouse held suspended by the tail next to a table edge. The mouse is slowly advanced toward the edge of the table with its torso. A mouse without injury would extend its upper torso and paws simultaneously to reach the edge of the table. The baton test is done with the mouse held suspended by the tail and allowed to grasp a 5-mm diameter stick with its forelimbs. After the mouse grasps the applicator, it is released while the mouse remains suspended. A mouse without injury would grasp the applicator with both forelimbs. For both tests, following unilateral lesion, we will be able to differentiate between the unlesioned and the lesioned side. Each test will be scored between 0 and 2 with 0 being both limbs extending/grabbing and 2 being no response from the injured paw. The timeline of these tests differs from the study of the detour circuit as a baseline and a post injury time point are necessary (Figure 15a). The forelimb placing test will assess recovery of proprioception, sensory input as well as coordination, the baton test for proprioception and coordination.

The forelimb placing test showed an injury effect two days post lesion (Figure 15b, $p<0.001$ injured 2d vs injured baseline) as well as no significant difference between lesioned and unlesioned groups 12 weeks post lesion. Additionally, a significant difference

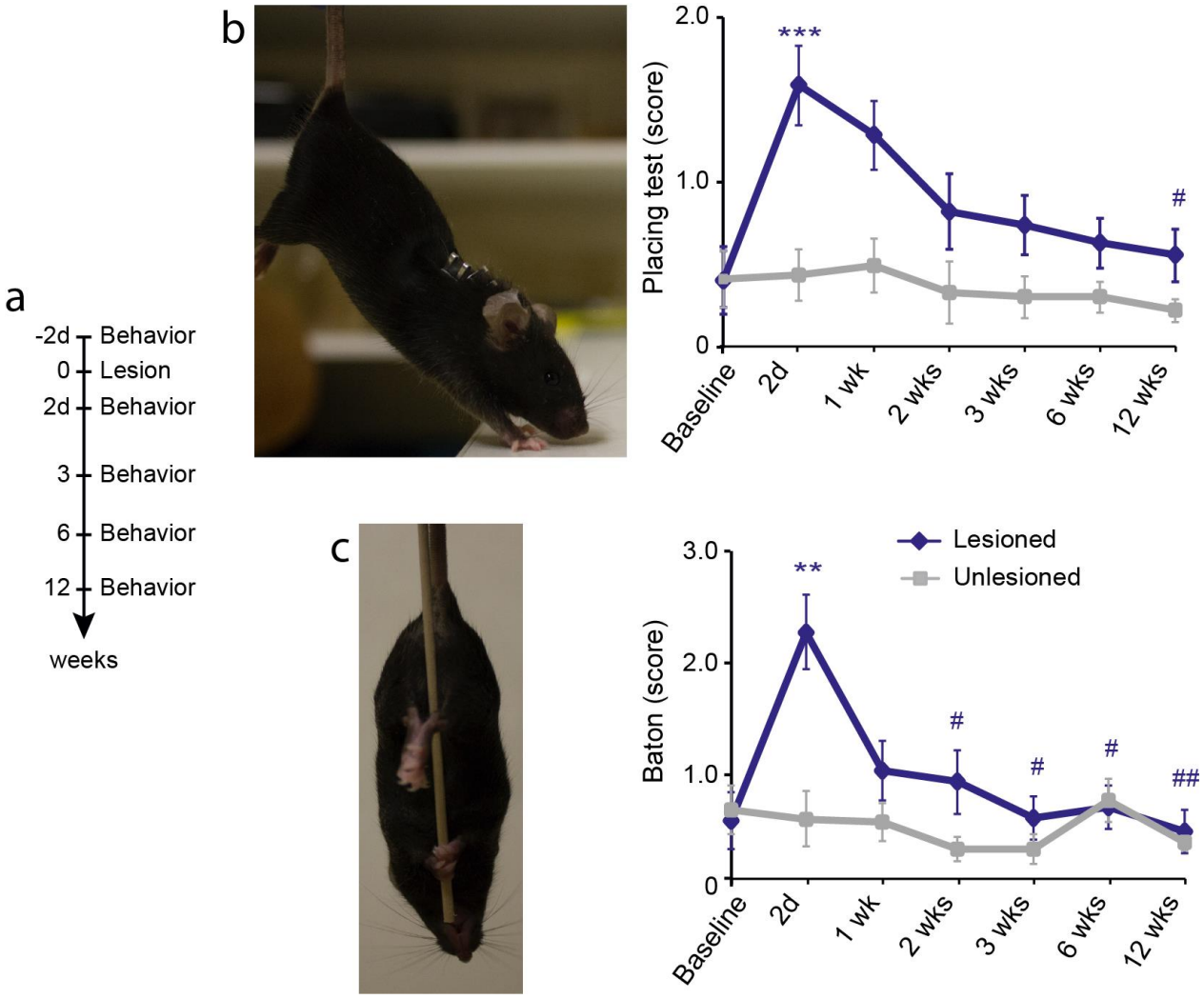

Figure 15 ***Spontaneous proprioceptive recovery following dorsal column lesion****. (a) Timeline of the dorsal column lesion paradigm and behavioral testing. (b) Picture of the forelimb pacing test and quantitative analysis of the scores obtained at baseline and different timepoints post dorsal column lesion. (c) Picture of the Baton test and quantitative analysis of the scores obtained at baseline and different timepoints post dorsal column lesion. Datasets were first tested for normality (non-normal distribution) and then analyzed using repeated nonparametric ANOVA (Friedmann test) followed by post-hoc multiple comparison Dunn's tests. n=12-13 per group. *** p<0.001: 2dpi injured vs baseline injured, ** p<0.01: 2dpi injured vs baseline injured. ## p<0.01: 12wks injured vs 2dpi injured, # p<0.05: 12wks injured vs 2dpi injured from (Granier et al., 2020)*

was observed between 12 weeks and 2 dpi (Figure 15b, $p<0.05$ 12wks injured vs 2dpi injured). A weaker injury effect is observed for the baton test (Figure 15c, $p<0.01$ injured 2d vs injured baseline) but contrarily to the forelimb placing response, this test showed significant improvement as early as 3 weeks post lesion (Figure 15c, $p<0.05$ and $p<0.01$ 3, 6, and 12wks injured vs 2dpi injured).

These findings showed that the detour circuit formed between the DRG and the cuneate nucleus allow the sensory and proprioceptive inputs to recover almost fully 12 weeks after the injury.

The interneurons responsible for this spontaneous recovery are nevertheless not known.

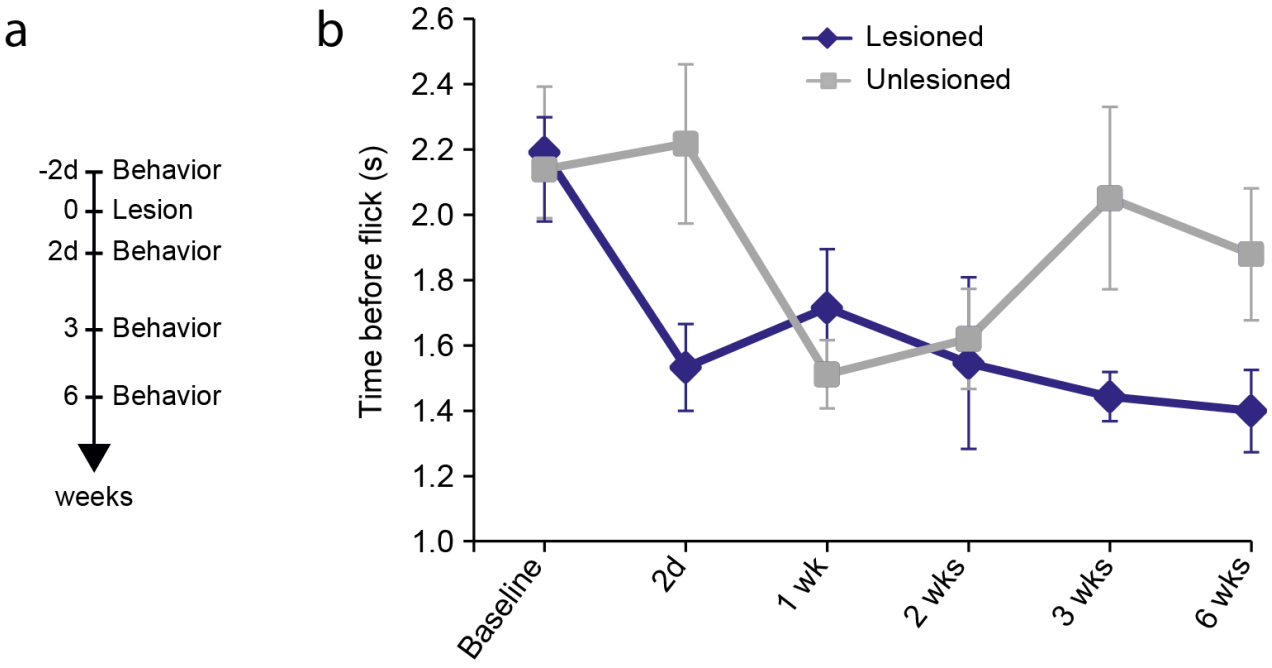

Figure 16 ***Dorsal column lesion doesn't induce nociception*** *(a) Timeline of the dorsal column lesion paradigm and behavioral testing. (b) Quantitative analysis of the response time obtained at baseline and different timepoints post dorsal column lesion in the tail flick test. n=12-13 per group.*

In order to look at nociception, the tail flick test was performed. In brief, mice were held in a tube and their tail was put in a warm water bath (temperature between 46 and 52 degrees) until flicking. The timeline of this experiment (Figure 16a) differed from the sensory tests as it was shown mice tend to habituate when too often performed. The response time was used as readout (Figure 16b). We observed huge disparities between groups as well as between mice, but no significant difference was shown between

lesioned and unlesioned groups. These data are however to be taken carefully as the tail flick test was shown to be regulated by environmental parameters such as room humidity or animal's body temperature. Nevertheless, no obvious aberrant pain was observed during the study.

IV. Characterization of interneurons reveals increase contact onto parvalbumine and glycinergic neurons.

Master thesis work from Angelina Fourli

Because of the difference of localization of the DRG collaterals as well as the contacted cuneate nucleus neurons, we hypothesized that different types of interneurons might be recruited. One of the main challenges of this study was the combination of fluorescent dyes we had to use and the limitation of the confocal technology. Because of the AAV expressing EYFP and the rabies mcherry, we had to use the fluorescence still available: EGFP and far red. Luckily, two transgenic mice lines were available for us to use and were expressing EGFP in either glycinergic (GlyT2) or GABAergic cells (GAD). In order to label Parvalbumine (PV), a subtype of GABAergic cells, glutaminase, for excitatory neurons, and CGRP, a known neurotransmitter implicated in nociception, immunohistochemistry staining was performed. Parvalbumine neurons are known to be implicated in proprioception, making them a probable target of DRG collaterals (de Nooij *et al*, 2013).

First, we looked at overall population of cuneate nucleus neurons and saw that all markers were expressed. The same observation was done in the population of contacted cuneate nucleus projecting neurons, even if CGRP and GAD positive cells were almost non-

existent (Figure 18). Moreover, no significant change in these two neuronal populations was observed following dorsal column lesion.

One of the questions we had following localization of the cuneate nucleus projecting neurons was whether a change in neuronal population might trigger the sprouting of the DRG collaterals. Therefore, we looked at the number of PV and GlyT2 positive neurons that were contacted post lesion and compared it the control group (Figure 17).

First, we saw that in an unlesioned mouse, glutaminase positive neurons were more contacted than PV or GlyT2 positive ones (0,45 vs 0,2 and 0,18 respectively). Post lesion (3 or 12 weeks), no significant difference was observed. It should be noted that no change in glutaminase positive neurons was observed between control and lesioned animal (Figure 17a). We saw previously that following dorsal column lesion, a refinement between 3 and 12 weeks happened. Nevertheless, no significant change in neuronal population was this time seen.

The major changes were observed in PV and GlyT2 positive cells (Figure 17b and c). Following dorsal lesion, a three-fold increase in PV positive contacted neurons was detected, 3 weeks post lesion (2.5-fold 12 weeks post injury) and a 2.5-fold increase in GlyT2 positive cells (at both 3 and 12 weeks timepoints).

As previously done, the number of contacts onto cuneate nucleus projecting neurons was assessed for each neuronal population. As per the number of contacted neurons, no significant change in number of contacts onto glutaminase positive neurons was observed. Similarly, to the number of PV positive contacted neurons, a significant increase in number of contacts was seen, in both 3- and 12-weeks groups (Figure17b, right).

One difference was nevertheless noticed: following dorsal column lesion, the number of contacts onto GlyT2 positive neurons significantly increase but was lost 12 weeks post lesion (Figure 17c, right). It should be however kept in mind that the total number of contacted GlyT2 positive neurons was in this group still significantly increased.

The number of contacts onto CPRG and GAD positive neurons was close to non-existent as these two populations were barely contacted by DRG collaterals.

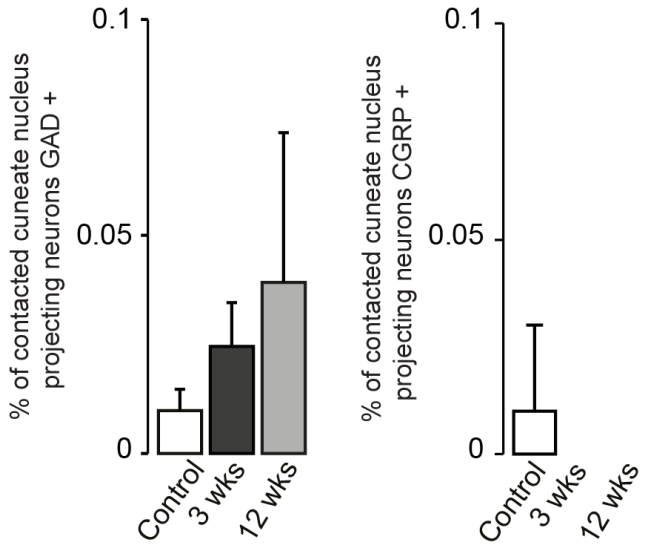

Figure 17 ***Characterization of cuneate nucleus projecting neurons.*** *Graphs indicating the percentage of cuneate nucleus projecting neurons positive for GAD and CGRP.*

All these results showed us that following dorsal column lesion, DRG collaterals target specific neuronal populations in order to form the detour circuit. As stated before,

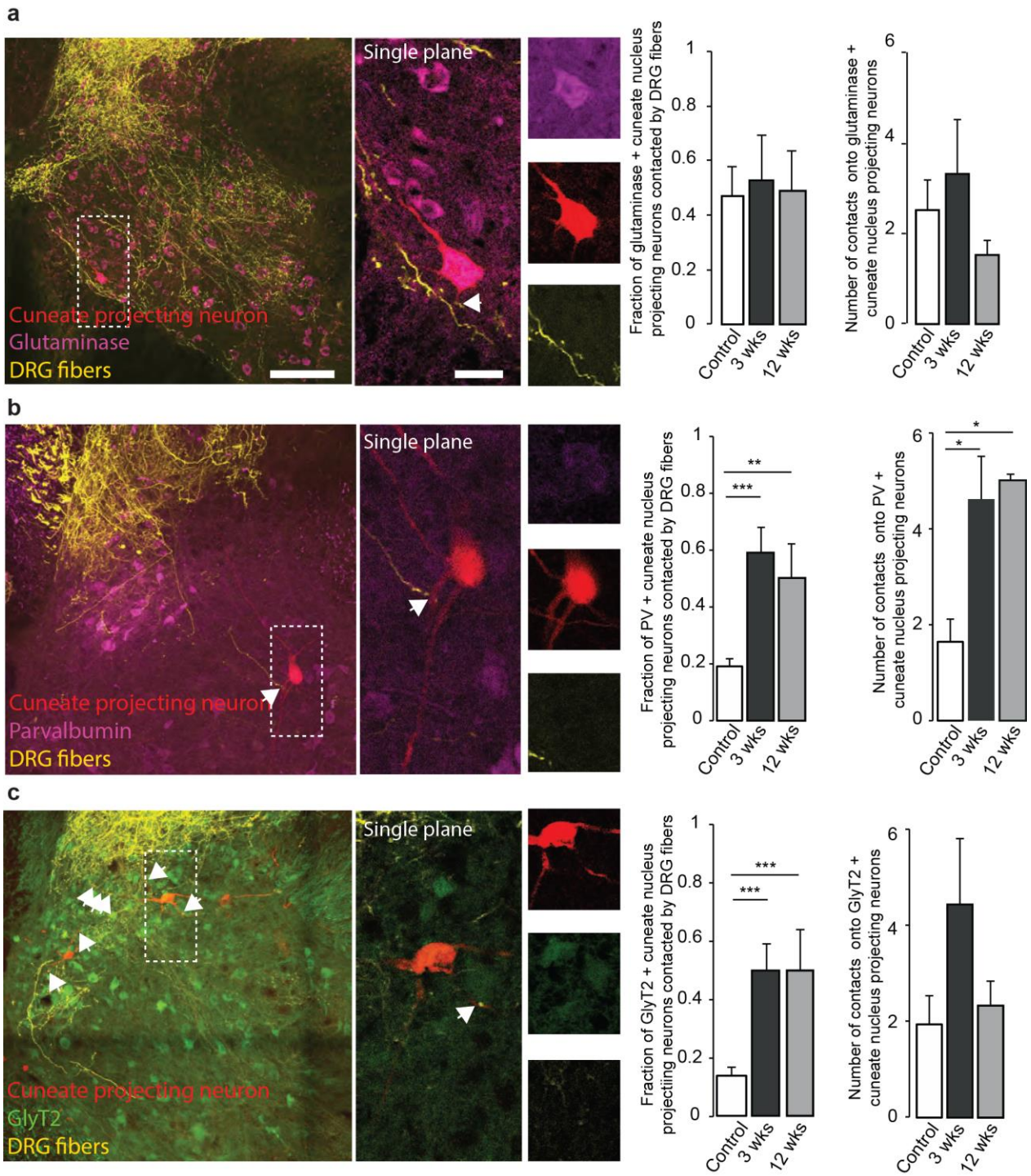

Figure 18 ***Characterization of the nature of the cuneate nucleus relay projecting relay neurons****. (a) Confocal images of cuneate nucleus neurons (red) double-labeled with markers for glutaminase (purple). Quantification of the % of cuneate nucleus projecting neurons immunoreactive for glutaminase contacted by DRG fibers (left) and quantification of the number of contacts onto glutaminase positive cuneate projecting neurons (right). (b) Confocal images of cuneate nucleus projecting neurons (red) double-labeled with markers for parvalbumin (purple). Quantification of the % of cuneate nucleus projecting neurons immunoreactive for parvalbumin contacted by DRG fibers (left) and quantification of the number of contacts onto parvalbumin positive cuneate projecting neurons (right). (c) Confocal images of cuneate nucleus projecting neurons (red) and transgenic labeling for glycinergic neurons (GlyT2: green). Quantification of the % of cuneate nucleus projecting neurons immunoreactive for glycine contacted by DRG fibers (left) and quantification of the number of contacts onto glycine positive cuneate projecting neurons (right). Areas boxed in the low magnification images are magnified 4 times in the left inset. All DRG fibers appear yellow on the pictures. Data were tested for normality and analyzed then with a one-way ANOVA followed by Dunnett's post-hoc test. N = 9 sections per group and n = 3 animal per group. ***: p <0.0001, **: p < 0.001, * p<0.01. Scale bar equal 40 µm in (a–e). For insets scale bar equals 10 µm in (a–e). from (Granier et al., 2020)*

parvalbumin neurons are known to be implicated in proprioception, making therefore this new circuit able to relay sensory and proprioceptive inputs back to the thalamus.

If this new circuit is able to relay sensory inputs, does it keep its specificity and does it still run through the same pathway?

V. The formation of a new circuit following dorsal lesion still rely on the dorsal medial lemniscus pathway

One information was still missing after the validation of the formation of the detour circuit: is the dorsal medial lemniscus pathway responsible for the spontaneous recovery.

In order to assess this question, we performed a relesion on mice 12 weeks post dorsal column lesion and performed again the behavioral tests (forelimb placing response and baton test). The unlesioned group was kept as control through this experiment (Figure 19a).

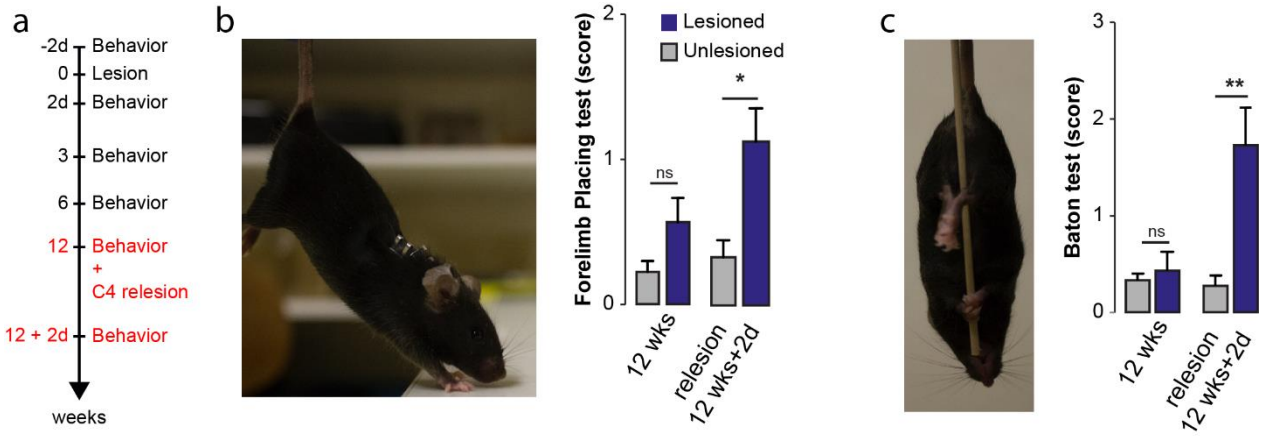

Figure 19 ***Formation of the detour circuit mediates functional recovery.*** *(a) Timeline of the dorsal column lesion paradigm and behavioral testing. (b) Picture of the forelimb pacing test and quantitative analysis of the scores obtained at 12 weeks as well as 2 days post relesion (c) Picture of the Baton test and quantitative analysis of the scores obtained at 12 weeks as well as 2 days post relesion. Datasets were first tested for normality (non-normal distribution) and then analyzed using a Kruskall-Wallis test followed by post-hoc multiple comparison Dunn's tests ** p<0.001, * p<0.01. n=12 in the unlesioned group and 13 in the lesioned group.*

The new lesion was performed at level C6 just above the DRG where contact formation between collaterals and cuneate nucleus projecting neurons was seen. Following the relesion, both forelimb and baton test showed a lesion effect and a significant worsening of the score (Figure 19b and c). It should be noted that this new lesion effect did not reach the same level as the first lesion.

These data led us to conclude on the implication of the dorsal medial lemniscus pathway in the detour circuit formation following a sensory lesion and its ability to restore proprioceptive inputs.

Chapter 5 Discussion

This study began after the detour circuit paradigm was found (Bareyre *et al.*, 2004). Bareyre et al. observed that following thoracic hemisection, the corticospinal tract was able to spread collaterals in the ventral layers of the spinal cord to contact long propriospinal neurons which would then contact motor neurons in the lumbar spinal cord. Other studies followed, showing the same results, or studying the same paradigm in other tracts (Ahuja *et al.*, 2017; Courtine *et al.*, 2009; Gros *et al.*, 2010). It was then hypothesized that the motor tracts were not the only ones who could remodel following injury. Moreover, motor recovery in spinal cord patients has been shown to be strongly correlated with sensory recovery. Additionally, Hollis II et al. showed plasticity of sensory axons (Hollis *et al.*, 2015). This study tried therefore to elucidate if sensory tracts and axons remodel following injury, if reorganization of the tract implicate a new population of relay neurons and if the formation of a new detour circuit allows functional recovery.

I. Study of the DRG sprouting following dorsal column lesion

As a beginning for this study, only the response of DRG neurons following dorsal column lesion was assessed. The lesion was performed at cervical level 2 and was let 3 or 12 weeks to recover. Ten days prior to sacrifice, an adeno-associated virus expressing EGFP was injected in the DRG at level cervical 6 to label the ascending tract.

The results first showed a difference between the motor and sensory system. The dorsal column tract spreads collaterals in the grey matter of the spinal cord even unlesioned. It shows how versatile and adaptive the sensory system is and led to further elucidate this

hypothesis. We saw that following injury, the DRG neurons spread significantly more collaterals in the spinal cord, probably trying to counteract the loss of sensory input above the lesion. One interesting observation was the decrease of collaterals 12 weeks post lesion, resembling what happens in the motor system (Bareyre *et al.*, 2004; Jacobi & Bareyre, 2015; Lang *et al.*, 2012). This decrease can be seen as refinement of already formed connections where aberrant contacts are lost to those triggering functional recovery.

We then looked more into detail at these collaterals and if their varicosities might spread differently after injury or even if the refinement 12 weeks post lesion might be the result of change of target. We saw that the number of varicosities in the intermediate layers of the spinal cord did not change after lesion but did increase significantly in ventral and dorsal layers at 3 and 12 weeks. Not only an increase in exiting collaterals was observed, but as well an increase in number of varicosities, hypothetically synapses, that could therefore contact neurons to regenerate the lost connections.

Our conclusion was that following dorsal column lesion, the DRG axons are able to reroute their axons, spread more in the spinal cord and form more varicosities, in hope to find meaningful connections to restore the pathway.

II. Study of the cuneate nucleus neurons and how they get contacted by DRG collaterals

After we saw that DRG neurons were able to spread in the spinal cord following injury, we wanted to look more into detail at the neurons that were contacted by these collaterals. The dorsal column pathway travels from the DRG to the medulla oblongata to finally send

proprioceptive inputs in the thalamus (Kandel *et al.*, 2000). The DRG neurons contact cuneate nucleus projecting neurons (their postsynaptic contacts) through two pathways. The first, through a direct connection to the cuneate nucleus, conveys about 80% of the overall sensory inputs. The second, through contact onto relay neurons which then contact cuneate nucleus neurons, relays about 20% of the inputs.

In order to label cuneate nucleus projecting neurons, we used a pseudotyped rabies virus that allowed to only label first degree connections. Shortly, the rabies virus is cloned without its glycoprotein and can't therefore travel through synapses (Mebatsion *et al.*, 1996). Once the rabies virus is complemented, it can travel retrogradely, making the fluorescence visible in the first-degree neurons. One advantage of this technique is the ability to follow where the rabies virus entered (because it will label the cell it first infected), where the G protein virus entered (because this virus can as well be marked with a fluorescent protein) and which neuron is contacting the primary cell. In our study, this allowed us to assess successful injection in the cuneate nucleus: when the rabies virus is injected with the G-protein, it will travel through the intact dorsal tract and label the DRG.

After successful labeling of the cuneate nucleus projecting neurons, we wondered if any change in localization happened following injury, as we previously saw that DRG collaterals had more varicosities and were differently localized. We could see that 3 weeks and even stronger 12 weeks post injury, the cuneate nucleus projecting neurons were increased in the ventral layers of the spinal cord. Once these neurons were contacted by DRG collaterals, this difference was only true 12 weeks post lesion. Taking the overall population of cuneate nucleus projecting neurons, only 20% of them got contacted in a control mouse. After lesion, this number significantly increased to 40% but decreased

again 12 weeks post injury, probably resulting from a refinement of immature connections. Our ability to image simple plane in a spinal cord section allowed us to look at single contact between DRG collaterals and cuneate nucleus projecting neurons. Using this technique, we observed that both the total number of contact as well as the number of contacts per cuneate nucleus projecting neurons increase significantly 3 weeks post lesion and was sustained after 12 weeks.

Our conclusion was that following injury, the DRG collaterals contact cuneate nucleus projecting neurons in order to restore the pathway. These collaterals will increase both the number of neurons as well as the number of contacts onto each of them, strengthening the valuable connections and establishing new ones to relay the sensory and proprioceptive inputs.

III. Study of the functional recovery

Functional recovery has always been the primary readout after spinal cord injury. When spared tissue is left to recover, and a new circuit is forming, one hope is that it will lead to functional recovery. In the motor system, it was shown in mice and rats that spontaneous rerouting of the CST lead to improvement on behavioral tests such as the catwalk and the ladder run (Jacobi & Bareyre, 2015; Loy *et al.*, 2018; Metz & Whishaw, 2009). Other behavioral tests have been used to assess motor recovery: the treadmill, the reaching task and the BBB scale (Ahmed *et al*, 2019; Courtine *et al.*, 2009). These tests look at both fine and gross motor skills and are able to show specific types of recovery. Following dorsal column lesion, other behavioral tests are required because no motor tracts have been damaged. In our study, we used the forelimb placing response, assessing recovery

of proprioception, sensory input as well as coordination and the baton test for proprioception and coordination (Shelton *et al.*, 2008).

In our study, we showed that following dorsal column lesion, mice performed worse 2 days post injury and recover through time. This lesion effect can be explained as the injury shock and explain why mice already recover a lot at one week post lesion. In the forelimb placing test, we saw that mice recovered slowly until 12 weeks, where no significant difference with the unlesioned group was seen. In the baton test, this result could be seen already 3 weeks after injury. This difference could be explained by the fact that the baton test assesses for tactile input and proprioception whereas the forelimb placing test for forelimb coordination as well. Proprioceptive and sensory inputs are transmitted back to the cuneate nucleus through mature connections between DRG axons and cuneate nucleus projecting neurons. With the baton and forelimb placing tests, we show that already 3 weeks post-lesion, mice recover sensory and proprioceptive inputs, triggered by the formation of the detour circuit.

One other aspect of sensory recovery still needs to be looked at: it is known that following spinal cord lesion, patients experience phantom pain, a phenomenon that up to now isn't fully understood. This pain comes from nociceptive receptors that were injured during the lesion. Following dorsal column lesion, we asked ourselves if the same applied. We therefore performed the tail flick test, where the tail of a mouse is put in water with a constant temperature between 46°C and 52°C and the time until it flicks is recorded (each mouse is measured 3 times and the average of all time is taken). Multiple nociceptive tests are available, one of the most used, the von Frey test (Deuis *et al.*, 2017). The rodent is placed in a closed cage with a mesh floor, the test consists in a single filament

perpendicularly applied to the plantar surface of the hind paw and left until the paw buckles. As previously stated, the tail flick test has been used in smaller settings to decrease the financial cost of such tests and might not, when studying complex pain mechanisms, be the most optimal. Others have been using this test in order to look, for example, at functional performances in rat following spinal cord injury (Pajoohesh-Ganji *et al*, 2010) and described too much variability to have a predictive value. Therefore, other tests, such as the CatWalk, are now being used to look at allodynia after spinal cord injury (Gabriel *et al*, 2009). In our case, its use allowed us to make sure that we didn't exacerbate pain mechanism following dorsal column lesion.

The tail flick test did not reveal any significant changes between the groups following dorsal column lesion. Nevertheless, the data should be taken with caution, as the spreading of the values is inconsistent within the same group and as unlesioned mice worsened their score in the middle of the study. This could be explained by external factors that influence this test, such as body temperature or even humidity level (Berge *et al*, 1988; Lichtman *et al*, 1993).

Our conclusion was that following dorsal column lesion, spontaneous and functional recovery is observed in mouse 3 weeks post injury. This recovery increases through time and shows that 12 weeks post injury, lesioned mice recover to the level of unlesioned mice in proprioception, coordination, and sensory input.

IV. Characterization of the relay neurons and the changes in contact of DRG collaterals

The difference of localization of contacted nucleus projecting neurons led us think that different subtypes of relay neurons were contacted. In order to label these neurons, two methods were used: transgenic mice and immunohistochemistry. Transgenic mice lines present the advantage of being ready to use: once the tracer injected, the mice sacrificed and cut, the labeling is present. Nevertheless, one marker can be expressed by multiple cell types and might therefore overcrowd the picture. GlyT2-EGFP mice express a green fluorescent protein in all cells expressing glycine transporter 2 and are shown to be expressed in cells responsible for locomotion, respiration, or vocalization (Rousseau *et al*, 2008; Zafra *et al*, 2017). GAD-EGFP mice express a green fluorescence in all cells expressing somatostatin (Todd, 2017). Somatostatin expressing neurons have been shown to be significant players in shaping activity and plasticity of the nervous system, therefore being of interest following spinal cord lesion (Liguz-Lecznar *et al*, 2016). These two markers allowed us to label inhibitory and excitatory neurons in the spinal cord. We then used immunohistochemistry to label other subtypes of relay neurons: parvalbumin for neurons implicated in proprioception, CGRP for nociception and glutaminase for excitatory neurons (Cangro *et al*, 1984; Neugebauer *et al*, 2009).

We first saw that almost no DRG collaterals contacted neurons expressing CGRP, somehow confirming the result of the tail flick test, and showing no increase in pain related stimulus following dorsal column lesion. Additionally, close to no GAD positive cuneate nucleus projecting neurons were contacted. Interestingly, we found that DRG collaterals were mostly contacting glutaminase positive cuneate nucleus projecting neurons both in control and lesioned groups. Following dorsal column lesion, no significant change in

excitatory neurons recruitment was observed. The same observation was made for the number of contacts onto glutaminase expressing cuneate nucleus projecting neurons.

On another side, following injury, a significant increase of parvalbumin expressing neurons was observed. Almost three times more neurons were contacted by DRG collaterals at both 3 and 12 weeks timepoints. It showed that the recovery observed in the forelimb placing and baton test might be the result of increase contact between DRG neurons and proprioceptive neurons. Moreover, the number of contacts onto PV positive cuneate nucleus projecting neurons was more than doubled 3 weeks post injury and sustained at 12 weeks. It shows that the connections established at 3 weeks post injury are strengthened through time in order to relay sensory and proprioceptive inputs. Moreover, Parvalbumine expressing neurons have been shown to have a critical role in inhibition of sensory threshold, therefore coordinating the activity of neuronal ensemble. Additionally, in an experiment specifically simulating Parvalbumine inhibitory neurons, Petitjean et al. showed a decrease of pain responses resulting from a prevention mechanism inactivating pain circuits.

Neurons expressing glycine transporter 2 were as well significantly more contacted by DRG collaterals following injury. This 3-fold increase was observed 3- and 12-weeks post lesion and might show some level of neuronal excitability due to injury. It should be noted that glycinergic neurons control pain transmission as well in the dorsal spinal cord (Zafra *et al.*, 2017). An increase in number of contacts was as well observed 3 weeks post lesion but not sustained after 12 weeks. This result could mean that the recruitment of GlyT2 expressing neurons is necessary early after the injury but once the refinement over, they might not be as useful for recovery as parvalbumin expressing neurons.

Our conclusion was that DRG collaterals target primarily glutaminase expressing neurons but following a dorsal column lesion, they recruit new relay neurons expressing parvalbumin, which are responsible for relaying proprioceptive inputs.

V. Study of the implication of the dorsal column lemniscus pathway following recovery

We showed that following dorsal column lesion, mice were able to recovery proprioception and sensory inputs 12 weeks post injury. DRG neurons and cuneate nucleus form part of the dorsal column pathway (Kandel *et al.*, 2000) and are able to create a detour circuit following injury. The last question we had was whether following spinal reorganization, is the dorsal column pathway still relaying the sensory and proprioceptive inputs. In order to answer, a relesion experiment was conducted. Twelve weeks post injury, the lesioned mice were reopened, and a new dorsal column lesion was performed at cervical C6, where the DRG collaterals were previously contacting new relay neurons. We saw that after the relesion, mice in the injured group performed poorly the forelimb placing and baton tests. There was no significant difference between the score post lesion and post relesion even if the effect was to a lesser extent, showing that the new detour circuit formed was responsible for the functional recovery of proprioceptive and sensory input.

This study was able to show that following dorsal column lesion, the DRG neurons were able to send collaterals to cuneate nucleus projecting neurons. These collaterals targeted parvalbumin expressing neurons, responsible for the relay of proprioceptive stimuli and allowed functional recovery 12 weeks post injury. The recovery of sensory inputs might be of great relevance for patients with incomplete spinal cord injury in order to trigger and enhance motor recovery.

Chapter 6 Conclusion

In summary, I can conclude from this thesis:

Following dorsal column lesion, DRG neurons are able to spread collaterals in the grey matter of the spinal cord and reach more predominantly the dorsal and ventral layers of the spinal cord. These collaterals are established already 3 weeks post injury, refined but sustained 12 weeks after lesion. These collaterals reach and contact cuneate nucleus projecting neurons in the dorsal and intermediate layers of the spinal cord in unlesioned mice and 3 weeks post injury and primarily in intermediate layers 12 weeks after lesion. A significant increase in number of contacted cuneate nucleus projecting neurons as well as contacts onto these neurons is observed. The formation of a detour circuit allows functional recovery and of proprioception, coordination, and sensory inputs 12 weeks after injury without eliciting aberrant pain. This detour circuit formation is mediated by contact between DRG collaterals and cuneate nucleus projecting neurons expressing parvalbumin and glycine transporter 2. The functional recovery can be lost again after re-lesion of the tract above the previous injury.

The dorsal medial lemniscus tract can, like motor tract, recover following spinal cord injury, and might help patients fully recover after suffering from an incomplete lesion

.

Acknowledgements

First, I would like to thank Dr Florence Bareyre. Thank you for allowing me to work in your team even if I didn't look like the perfect candidate for the job, I hope I proved you wrong. Thank you as well for always being there when I needed help both work and private related. And to finish, thank you for being a part of the French culture that I never thought I would have in Munich and who made me in time of crisis, a little happier.

I would like to thank Pr. Kerschensteiner for his help and constructive remarks during my progress reports and TAC meetings. Thank you to Dr Ninkovic for being part of my TAC Committee, for always giving new ideas and constructive remarks as well as allowing me to collaborate on a great project.

I would like to thank the Bareyre and Kerschensteiner Lab for being there when I needed help, particularly Anne for showing me most of your surgery techniques as well as being a friend. I wish you all the best for your US adventure. Thank you, Elisa and Ola for showing me that there is something else outside the lab. Thank you, Elina, for being such a great Master student and for the amazing work you did, I would not have finished it without you, I wish you all the best for the end of your PhD as well as with your daughter. Thank you Almir for taking over when I wasn't in the lab and for making me laugh when I needed it the most.

Ich muss mich auch bei meinem Partner/Mann bedanken. Du warst immer da, wenn ich es brauchte, auch wenn ich nicht so einfach war. Diese Dissertation gehört dir auch ein bisschen, für alles dass du für unsere Familie getan hast. Ich liebe dich mehr.

Je voudrais aussi remercier toute ma famille, en particulier ma Maman et mon Papa. Merci de toujours avoir été là pour moi, de m'avoir soutenu mais aussi de m'avoir fait comprendre de quoi j'étais capable. Je vous aime infiniment. Je remercie aussi mes petites sœurs Emeline et Eve, pour être la quand j'ai besoin de parler et pour être des tatas formidables.

Je remercie aussi mes filles, Joséphine et Adeline. Pour être ma motivation de tous les jours même si vous être parfois la raison d'en avoir besoin.

Pour finir, je voudrais dédicacer cette thèse à ma grande sœur Cindy. Sans toi, je n'y serais jamais arrivé. Merci de m'avoir aidé, autant moralement que financièrement pendant mes années d'école d'ingénieur et de m'avoir poussé à partir faire ma thèse à Munich. Tu me montres encore et toujours que tu crois en moi bien plus que je ne crois en moi-même, j'admire ta ténacité et espère pouvoir te rendre fière d'être ta petite sœur. Encore mille mercis, je t'aime plus que je n'aie de mots pour le dire.

Bibliography

Ahmed RU, Alam M, Zheng YP (2019) Experimental spinal cord injury and behavioral tests in laboratory rats. *Heliyon* 5: e01324

Ahuja CS, Nori S, Tetreault L, Wilson J, Kwon B, Harrop J, Choi D, Fehlings MG (2017) Traumatic Spinal Cord Injury-Repair and Regeneration. *Neurosurgery* 80: S9-S22

Al-Chalabi M, Reddy V, Alsalman I (2020) Neuroanatomy, Posterior Column (Dorsal Column). In: *StatPearls*, Treasure Island (FL)

Allen AR (1911) Surgery of experimental lesion of spinal cord equivalent to crush injury of fracture dislocation of spinal column: a preliminary report. *Journal of the American Medical Association* LVII: 878-880

Anderson DK, Waters TR, Means ED (1988) Pretreatment with alpha tocopherol enhances neurologic recovery after experimental spinal cord compression injury. *J Neurotrauma* 5: 61-67

Bareyre FM, Kerschensteiner M, Raineteau O, Mettenleiter TC, Weinmann O, Schwab ME (2004) The injured spinal cord spontaneously forms a new intraspinal circuit in adult rats. *Nat Neurosci* 7: 269-277

Behrman AL, Harkema SJ (2000) Locomotor training after human spinal cord injury: a series of case studies. *Phys Ther* 80: 688-700

Berge OG, Garcia-Cabrera I, Hole K (1988) Response latencies in the tail-flick test depend on tail skin temperature. *Neurosci Lett* 86: 284-288

Blesch A, Tuszynski MH (2003) Cellular GDNF delivery promotes growth of motor and dorsal column sensory axons after partial and complete spinal cord transections and induces remyelination. *J Comp Neurol* 467: 403-417

Blight AR, Young W (1989) Central axons in injured cat spinal cord recover electrophysiological function following remyelination by Schwann cells. *J Neurol Sci* 91: 15-34

Bracken MB, Holford TR (1993) Effects of timing of methylprednisolone or naloxone administration on recovery of segmental and long-tract neurological function in NASCIS 2. *J Neurosurg* 79: 500-507

Brambilla R, Bracchi-Ricard V, Hu WH, Frydel B, Bramwell A, Karmally S, Green EJ, Bethea JR (2005) Inhibition of astroglial nuclear factor kappaB reduces inflammation and improves functional recovery after spinal cord injury. *J Exp Med* 202: 145-156

Braughler JM (1985) Lipid peroxidation-induced inhibition of gamma-aminobutyric acid uptake in rat brain synaptosomes: protection by glucocorticoids. *J Neurochem* 44: 1282-1288

Burns SP, Golding DG, Rolle WA, Jr., Graziani V, Ditunno JF, Jr. (1997) Recovery of ambulation in motor-incomplete tetraplegia. *Arch Phys Med Rehabil* 78: 1169-1172

Cameron EG, Xia X, Galvao J, Ashouri M, Kapiloff MS, Goldberg JL (2020) Optic Nerve Crush in Mice to Study Retinal Ganglion Cell Survival and Regeneration. *Bio Protoc* 10

Cangro CB, Sweetnam PM, Neale JH, Haser WG, Curthoys NP (1984) Selective localization of glutaminase in spinal and sensory nerve cells. A potential marker for glutamate neurotransmission. *JAMA* 251: 797

Cardenas DD, Jensen MP (2006) Treatments for chronic pain in persons with spinal cord injury: A survey study. *J Spinal Cord Med* 29: 109-117

Castro MJ, Apple DF, Jr., Rogers S, Dudley GA (2000) Influence of complete spinal cord injury on skeletal muscle mechanics within the first 6 months of injury. *Eur J Appl Physiol* 81: 128-131

Chang HT (2007) Subacute human spinal cord contusion: few lymphocytes and many macrophages. *Spinal Cord* 45: 174-182

Courtine G, Gerasimenko Y, van den Brand R, Yew A, Musienko P, Zhong H, Song B, Ao Y, Ichiyama RM, Lavrov I *et al* (2009) Transformation of nonfunctional spinal circuits into functional states after the loss of brain input. *Nat Neurosci* 12: 1333-1342

Cramer SC, Lastra L, Lacourse MG, Cohen MJ (2005) Brain motor system function after chronic, complete spinal cord injury. *Brain* 128: 2941-2950

Curt A, Schwab ME, Dietz V (2004) Providing the clinical basis for new interventional therapies: refined diagnosis and assessment of recovery after spinal cord injury. *Spinal Cord* 42: 1-6

Curtis R, Green D, Lindsay RM, Wilkin GP (1993) Up-regulation of GAP-43 and growth of axons in rat spinal cord after compression injury. *J Neurocytol* 22: 51-64

David S, Aguayo AJ (1981) Axonal elongation into peripheral nervous system "bridges" after central nervous system injury in adult rats. *Science* 214: 931-933

de Nooij JC, Doobar S, Jessell TM (2013) Etv1 inactivation reveals proprioceptor subclasses that reflect the level of NT3 expression in muscle targets. *Neuron* 77: 1055-1068

Deuis JR, Dvorakova LS, Vetter I (2017) Methods Used to Evaluate Pain Behaviors in Rodents. *Front Mol Neurosci* 10: 284

Dolinak D, Balraj E (2007) Autonomic dysreflexia and sudden death in people with traumatic spinal cord injury. *Am J Forensic Med Pathol* 28: 95-98

Dumont RJ, Okonkwo DO, Verma S, Hurlbert RJ, Boulos PT, Ellegala DB, Dumont AS (2001a) Acute spinal cord injury, part I: pathophysiologic mechanisms. *Clin Neuropharmacol* 24: 254-264

Dumont RJ, Verma S, Okonkwo DO, Hurlbert RJ, Boulos PT, Ellegala DB, Dumont AS (2001b) Acute spinal cord injury, part II: contemporary pharmacotherapy. *Clin Neuropharmacol* 24: 265-279

Dykstra DD, Sidi AA, Scott AB, Pagel JM, Goldish GD (1988) Effects of botulinum A toxin on detrusor-sphincter dyssynergia in spinal cord injury patients. *J Urol* 139: 919-922

Edgerton VR, Roy RR (2009) Robotic training and spinal cord plasticity. *Brain Res Bull* 78: 4-12

Edgerton VR, Tillakaratne NJ, Bigbee AJ, de Leon RD, Roy RR (2004) Plasticity of the spinal neural circuitry after injury. *Annu Rev Neurosci* 27: 145-167

Eltorai I, Kim R, Vulpe M, Kasravi H, Ho W (1992) Fatal cerebral hemorrhage due to autonomic dysreflexia in a tetraplegic patient: case report and review. *Paraplegia* 30: 355-360

Faden AI, Wu J, Stoica BA, Loane DJ (2016) Progressive inflammation-mediated neurodegeneration after traumatic brain or spinal cord injury. *Br J Pharmacol* 173: 681-691

Fann JR, Bombardier CH, Richards JS, Wilson CS, Heinemann AW, Warren AM, Brooks L, McCullumsmith CB, Temkin NR, Warms C *et al* (2015) Venlafaxine extended-release for depression following spinal cord injury: a randomized clinical trial. *JAMA Psychiatry* 72: 247-258

Fann JR, Crane DA, Graves DE, Kalpakjian CZ, Tate DG, Bombardier CH (2013) Depression treatment preferences after acute traumatic spinal cord injury. *Arch Phys Med Rehabil* 94: 2389-2395

Fehlings MG, Perrin RG (2005) The role and timing of early decompression for cervical spinal cord injury: update with a review of recent clinical evidence. *Injury* 36 Suppl 2: B13-26

Fehlings MG, Tator CH, Linden RD (1989) The effect of nimodipine and dextran on axonal function and blood flow following experimental spinal cord injury. *J Neurosurg* 71: 403-416

Fehlings MG, Vaccaro A, Wilson JR, Singh A, D WC, Harrop JS, Aarabi B, Shaffrey C, Dvorak M, Fisher C *et al* (2012) Early versus delayed decompression for traumatic cervical spinal cord injury: results of the Surgical Timing in Acute Spinal Cord Injury Study (STASCIS). *PLoS One* 7: e32037

Finnerup NB, Sindrup SH, Bach FW, Johannesen IL, Jensen TS (2002) Lamotrigine in spinal cord injury pain: a randomized controlled trial. *Pain* 96: 375-383

Fouad K, Pedersen V, Schwab ME, Brosamle C (2001) Cervical sprouting of corticospinal fibers after thoracic spinal cord injury accompanies shifts in evoked motor responses. *Curr Biol* 11: 1766-1770

Gabriel AF, Marcus MA, Walenkamp GH, Joosten EA (2009) The CatWalk method: assessment of mechanical allodynia in experimental chronic pain. *Behav Brain Res* 198: 477-480

Gensel JC, Tovar CA, Hamers FP, Deibert RJ, Beattie MS, Bresnahan JC (2006) Behavioral and histological characterization of unilateral cervical spinal cord contusion injury in rats. *J Neurotrauma* 23: 36-54

Goldshmit Y, Lythgo N, Galea MP, Turnley AM (2008) Treadmill training after spinal cord hemisection in mice promotes axonal sprouting and synapse formation and improves motor recovery. *J Neurotrauma* 25: 449-465

Granier C, Schwarting J, Fourli E, Laage-Gaupp F, Hennrich AA, Schmalz A, Jacobi A, Wesolowski M, Conzelmann KK, Bareyre FM (2020) Formation of somatosensory detour circuits mediates functional recovery following dorsal column injury. *Sci Rep* 10: 10953

Grimm D, Kay MA (2003) From virus evolution to vector revolution: use of naturally occurring serotypes of adeno-associated virus (AAV) as novel vectors for human gene therapy. *Curr Gene Ther* 3: 281-304

Gros T, Sakamoto JS, Blesch A, Havton LA, Tuszynski MH (2010) Regeneration of long-tract axons through sites of spinal cord injury using templated agarose scaffolds. *Biomaterials* 31: 6719-6729

Guha A, Tator CH, Endrenyi L, Piper I (1987) Decompression of the spinal cord improves recovery after acute experimental spinal cord compression injury. *Paraplegia* 25: 324-339

Hains BC, Black JA, Waxman SG (2003) Primary cortical motor neurons undergo apoptosis after axotomizing spinal cord injury. *J Comp Neurol* 462: 328-341

Hall ED (1988) Effects of the 21-aminosteroid U74006F on posttraumatic spinal cord ischemia in cats. *J Neurosurg* 68: 462-465

Hall ED (1992) The neuroprotective pharmacology of methylprednisolone. *J Neurosurg* 76: 13-22

Hall ED (1993) Neuroprotective actions of glucocorticoid and nonglucocorticoid steroids in acute neuronal injury. *Cell Mol Neurobiol* 13: 415-432

Hamada Y, Ikata T, Katoh S, Tsuchiya K, Niwa M, Tsutsumishita Y, Fukuzawa K (1996) Roles of nitric oxide in compression injury of rat spinal cord. *Free Radic Biol Med* 20: 1-9

Hamers FP, Lankhorst AJ, van Laar TJ, Veldhuis WB, Gispen WH (2001) Automated quantitative gait analysis during overground locomotion in the rat: its application to spinal cord contusion and transection injuries. *J Neurotrauma* 18: 187-201

Heng C, de Leon RD (2009) Treadmill training enhances the recovery of normal stepping patterns in spinal cord contused rats. *Exp Neurol* 216: 139-147

Hollis ER, 2nd, Ishiko N, Pessian M, Tolentino K, Lee-Kubli CA, Calcutt NA, Zou Y (2015) Remodelling of spared proprioceptive circuit involving a small number of neurons supports functional recovery. *Nat Commun* 6: 6079

Hornby TG, Zemon DH, Campbell D (2005) Robotic-assisted, body-weight-supported treadmill training in individuals following motor incomplete spinal cord injury. *Phys Ther* 85: 52-66

Huang M, Chen H, Jiang C, Xie K, Tang P, Ou R, Zeng J, Liu Q, Li Q, Huang J *et al* (2016) Effects of botulinum toxin A injections in spinal cord injury patients with detrusor overactivity and detrusor sphincter dyssynergia. *J Rehabil Med* 48: 683-687

Hubli M, Dietz V (2013) The physiological basis of neurorehabilitation--locomotor training after spinal cord injury. *J Neuroeng Rehabil* 10: 5

Iaci JF, Vecchione AM, Zimber MP, Caggiano AO (2007) Chondroitin sulfate proteoglycans in spinal cord contusion injury and the effects of chondroitinase treatment. *J Neurotrauma* 24: 1743-1759

Inman DM, Steward O (2003) Ascending sensory, but not other long-tract axons, regenerate into the connective tissue matrix that forms at the site of a spinal cord injury in mice. *J Comp Neurol* 462: 431-449

Iwakura A, Dean J, Hamada H, Eaton E, Qin G, Losordo DW, Aikawa R (2005) Use of recombinant adeno-associated viral vectors as a tool for labeling bone marrow cells. *J Mol Cell Cardiol* 38: 799-802

Jacobi A, Bareyre FM (2015) Regulation of axonal remodeling following spinal cord injury. *Neural Regen Res* 10: 1555-1557

Jacobi A, Loy K, Schmalz AM, Hellsten M, Umemori H, Kerschensteiner M, Bareyre FM (2015) FGF22 signaling regulates synapse formation during post-injury remodeling of the spinal cord. *EMBO J* 34: 1231-1243

Jazayeri SB, Beygi S, Shokraneh F, Hagen EM, Rahimi-Movaghar V (2015) Incidence of traumatic spinal cord injury worldwide: a systematic review. *Eur Spine J* 24: 905-918

Jorgensen AY, Ahn J, Aboushaala K, Singh K (2015) Current concepts in the use of stem cells for the treatment of spinal cord injury. *Seminars in Spine Surgery* 27: 90-92

Kalpakjian CZ, Bombardier CH, Schomer K, Brown PA, Johnson KL (2009) Measuring depression in persons with spinal cord injury: a systematic review. *J Spinal Cord Med* 32: 6-24

Kandel ER, Schwartz JH, Jessell TM, Biochemistry Do, Jessell MBT, Siegelbaum S, Hudspeth A (2000) *Principles of neural science*. McGraw-hill New York

Kattenhorn LM, Tipper CH, Stoica L, Geraghty DS, Wright TL, Clark KR, Wadsworth SC (2016) Adeno-Associated Virus Gene Therapy for Liver Disease. *Hum Gene Ther* 27: 947-961

Khazaeipour Z, Taheri-Otaghsara SM, Naghdi M (2015) Depression Following Spinal Cord Injury: Its Relationship to Demographic and Socioeconomic Indicators. *Top Spinal Cord Inj Rehabil* 21: 149-155

Kim JE, Liu BP, Park JH, Strittmatter SM (2004) Nogo-66 receptor prevents raphespinal and rubrospinal axon regeneration and limits functional recovery from spinal cord injury. *Neuron* 44: 439-451

Kirshblum SC, Burns SP, Biering-Sorensen F, Donovan W, Graves DE, Jha A, Johansen M, Jones L, Krassioukov A, Mulcahey MJ *et al* (2011) International standards for neurological classification of spinal cord injury (revised 2011). *J Spinal Cord Med* 34: 535-546

Klugmann M, Symes CW, Leichtlein CB, Klaussner BK, Dunning J, Fong D, Young D, During MJ (2005) AAV-mediated hippocampal expression of short and long Homer 1 proteins differentially affect cognition and seizure activity in adult rats. *Mol Cell Neurosci* 28: 347-360

Krassioukov A, Warburton DE, Teasell R, Eng JJ, Spinal Cord Injury Rehabilitation Evidence Research T (2009) A systematic review of the management of autonomic dysreflexia after spinal cord injury. *Arch Phys Med Rehabil* 90: 682-695

Kuffler DP (2018) Origins of Phantom Limb Pain. *Mol Neurobiol* 55: 60-69

Lang C, Bradley PM, Jacobi A, Kerschensteiner M, Bareyre FM (2013) STAT3 promotes corticospinal remodelling and functional recovery after spinal cord injury. *EMBO Rep* 14: 931-937

Lang C, Guo X, Kerschensteiner M, Bareyre FM (2012) Single collateral reconstructions reveal distinct phases of corticospinal remodeling after spinal cord injury. *PLoS One* 7: e30461

Lavrov I, Gerasimenko YP, Ichiyama RM, Courtine G, Zhong H, Roy RR, Edgerton VR (2006) Plasticity of spinal cord reflexes after a complete transection in adult rats: relationship to stepping ability. *J Neurophysiol* 96: 1699-1710

Li GL, Brodin G, Farooque M, Funa K, Holtz A, Wang WL, Olsson Y (1996) Apoptosis and expression of Bcl-2 after compression trauma to rat spinal cord. *J Neuropathol Exp Neurol* 55: 280-289

Li Y, Walker CL, Zhang YP, Shields CB, Xu XM (2014) Surgical decompression in acute spinal cord injury: A review of clinical evidence, animal model studies, and potential future directions of investigation. *Front Biol (Beijing)* 9: 127-136

Lichtman AH, Smith FL, Martin BR (1993) Evidence that the antinociceptive tail-flick response is produced independently from changes in either tail-skin temperature or core temperature. *Pain* 55: 283-295

Liguz-Lecznar M, Urban-Ciecko J, Kossut M (2016) Somatostatin and Somatostatin-Containing Neurons in Shaping Neuronal Activity and Plasticity. *Front Neural Circuits* 10: 48

Lim JH, Jung CS, Byeon YE, Kim WH, Yoon JH, Kang KS, Kweon OK (2007) Establishment of a canine spinal cord injury model induced by epidural balloon compression. *J Vet Sci* 8: 89-94

Liu T, Xu J, Chan BP, Chew SY (2012) Sustained release of neurotrophin-3 and chondroitinase ABC from electrospun collagen nanofiber scaffold for spinal cord injury repair. *J Biomed Mater Res A* 100: 236-242

Louie DR, Eng JJ, Lam T, Spinal Cord Injury Research Evidence Research T (2015) Gait speed using powered robotic exoskeletons after spinal cord injury: a systematic review and correlational study. *J Neuroeng Rehabil* 12: 82

Loy K, Schmalz A, Hoche T, Jacobi A, Kreutzfeldt M, Merkler D, Bareyre FM (2018) Enhanced Voluntary Exercise Improves Functional Recovery following Spinal Cord Injury by Impacting the Local Neuroglial Injury Response and Supporting the Rewiring of Supraspinal Circuits. *J Neurotrauma* 35: 2904-2915

Ma M, Basso DM, Walters P, Stokes BT, Jakeman LB (2001) Behavioral and histological outcomes following graded spinal cord contusion injury in the C57Bl/6 mouse. *Exp Neurol* 169: 239-254

Marmigere F, Ernfors P (2007) Specification and connectivity of neuronal subtypes in the sensory lineage. *Nat Rev Neurosci* 8: 114-127

Martin D, Robe P, Franzen R, Delree P, Schoenen J, Stevenaert A, Moonen G (1996) Effects of Schwann cell transplantation in a contusion model of rat spinal cord injury. *J Neurosci Res* 45: 588-597

Masri R, Keller A (2012) Chronic pain following spinal cord injury. *Adv Exp Med Biol* 760: 74-88

McKinley WO, Jackson AB, Cardenas DD, DeVivo MJ (1999) Long-term medical complications after traumatic spinal cord injury: a regional model systems analysis. *Arch Phys Med Rehabil* 80: 1402-1410

McTigue DM (2008) Potential Therapeutic Targets for PPARgamma after Spinal Cord Injury. *PPAR Res* 2008: 517162

Mebatsion T, Konig M, Conzelmann KK (1996) Budding of rabies virus particles in the absence of the spike glycoprotein. *Cell* 84: 941-951

Metz GA, Whishaw IQ (2009) The ladder rung walking task: a scoring system and its practical application. *Journal of visualized experiments : JoVE*

Nas K, Yazmalar L, Sah V, Aydin A, Ones K (2015) Rehabilitation of spinal cord injuries. *World J Orthop* 6: 8-16

Naso MF, Tomkowicz B, Perry WL, 3rd, Strohl WR (2017) Adeno-Associated Virus (AAV) as a Vector for Gene Therapy. *BioDrugs* 31: 317-334

Neugebauer V, Galhardo V, Maione S, Mackey SC (2009) Forebrain pain mechanisms. *Brain Res Rev* 60: 226-242

Olsson Y, Sharma HS, Nyberg F, Westman J (1995) The opioid receptor antagonist naloxone influences the pathophysiology of spinal cord injury. *Prog Brain Res* 104: 381-399

Oyinbo CA (2011) Secondary injury mechanisms in traumatic spinal cord injury: a nugget of this multiply cascade. *Acta Neurobiol Exp (Wars)* 71: 281-299

Pajoohesh-Ganji A, Byrnes KR, Fatemi G, Faden AI (2010) A combined scoring method to assess behavioral recovery after mouse spinal cord injury. *Neurosci Res* 67: 117-125

Paterniti I, Genovese T, Crisafulli C, Mazzon E, Di Paola R, Galuppo M, Bramanti P, Cuzzocrea S (2009) Treatment with green tea extract attenuates secondary inflammatory response in an experimental model of spinal cord trauma. *Naunyn Schmiedebergs Arch Pharmacol* 380: 179-192

Raineteau O, Schwab ME (2001) Plasticity of motor systems after incomplete spinal cord injury. *Nat Rev Neurosci* 2: 263-273

Rivlin AS, Tator CH (1978) Effect of duration of acute spinal cord compression in a new acute cord injury model in the rat. *Surg Neurol* 10: 38-43

Rosenzweig ES, Courtine G, Jindrich DL, Brock JH, Ferguson AR, Strand SC, Nout YS, Roy RR, Miller DM, Beattie MS *et al* (2010) Extensive spontaneous plasticity of corticospinal projections after primate spinal cord injury. *Nat Neurosci* 13: 1505-1510

Rousseau F, Aubrey KR, Supplisson S (2008) The glycine transporter GlyT2 controls the dynamics of synaptic vesicle refilling in inhibitory spinal cord neurons. *J Neurosci* 28: 9755-9768

Saadoun S, Bell BA, Verkman AS, Papadopoulos MC (2008) Greatly improved neurological outcome after spinal cord compression injury in AQP4-deficient mice. *Brain* 131: 1087-1098

Sasaki M, Hains BC, Lankford KL, Waxman SG, Kocsis JD (2006) Protection of corticospinal tract neurons after dorsal spinal cord transection and engraftment of olfactory ensheathing cells. *Glia* 53: 352-359

Savic G, DeVivo MJ, Frankel HL, Jamous MA, Soni BM, Charlifue S (2017) Causes of death after traumatic spinal cord injury-a 70-year British study. *Spinal Cord* 55: 891-897

Schurch B, Stohrer M, Kramer G, Schmid DM, Gaul G, Hauri D (2000) Botulinum-A toxin for treating detrusor hyperreflexia in spinal cord injured patients: a new alternative to anticholinergic drugs? Preliminary results. *J Urol* 164: 692-697

Schurch B, Wichmann W, Rossier AB (1996) Post-traumatic syringomyelia (cystic myelopathy): a prospective study of 449 patients with spinal cord injury. *J Neurol Neurosurg Psychiatry* 60: 61-67

Schwab ME, Bartholdi D (1996) Degeneration and regeneration of axons in the lesioned spinal cord. *Physiol Rev* 76: 319-370

Sekhon LH, Fehlings MG (2001) Epidemiology, demographics, and pathophysiology of acute spinal cord injury. *Spine (Phila Pa 1976)* 26: S2-12

Sharif-Alhoseini M, Khormali M, Rezaei M, Safdarian M, Hajighadery A, Khalatbari MM, Safdarian M, Meknatkhah S, Rezvan M, Chalangari M *et al* (2017) Animal models of spinal cord injury: a systematic review. *Spinal Cord* 55: 714-721

Shelton SB, Pettigrew DB, Hermann AD, Zhou W, Sullivan PM, Crutcher KA, Strauss KI (2008) A simple, efficient tool for assessment of mice after unilateral cortex injury. *J Neurosci Methods* 168: 431-442

Siddall PJ, Loeser JD (2001) Pain following spinal cord injury. *Spinal Cord* 39: 63-73

Simon CM, Sharif S, Tan RP, LaPlaca MC (2009) Spinal cord contusion causes acute plasma membrane damage. *J Neurotrauma* 26: 563-574

Singh A, Tetreault L, Kalsi-Ryan S, Nouri A, Fehlings MG (2014) Global prevalence and incidence of traumatic spinal cord injury. *Clin Epidemiol* 6: 309-331

Smith CA, Chauhan BC (2018) In vivo imaging of adeno-associated viral vector labelled retinal ganglion cells. *Sci Rep* 8: 1490

Soden RJ, Walsh J, Middleton JW, Craven ML, Rutkowski SB, Yeo JD (2000) Causes of death after spinal cord injury. *Spinal Cord* 38: 604-610

Stys PK, Waxman SG, Ransom BR (1992) Ionic mechanisms of anoxic injury in mammalian CNS white matter: role of Na+ channels and Na(+)-Ca2+ exchanger. *J Neurosci* 12: 430-439

Teng YD, Wrathall JR (1997) Local blockade of sodium channels by tetrodotoxin ameliorates tissue loss and long-term functional deficits resulting from experimental spinal cord injury. *J Neurosci* 17: 4359-4366

Tetzlaff W, Okon EB, Karimi-Abdolrezaee S, Hill CE, Sparling JS, Plemel JR, Plunet WT, Tsai EC, Baptiste D, Smithson LJ *et al* (2011) A systematic review of cellular transplantation therapies for spinal cord injury. *J Neurotrauma* 28: 1611-1682

Todd AJ (2017) Identifying functional populations among the interneurons in laminae I-III of the spinal dorsal horn. *Mol Pain* 13: 1744806917693003

Valles M, Benito J, Portell E, Vidal J (2005) Cerebral hemorrhage due to autonomic dysreflexia in a spinal cord injury patient. *Spinal Cord* 43: 738-740

Vanicky I, Urdzikova L, Saganova K, Cizkova D, Galik J (2001) A simple and reproducible model of spinal cord injury induced by epidural balloon inflation in the rat. *J Neurotrauma* 18: 1399-1407

Wang X, Smith GM, Xu XM (2011) Preferential and bidirectional labeling of the rubrospinal tract with adenovirus-GFP for monitoring normal and injured axons. *J Neurotrauma* 28: 635-647

Wu B, Ren X (2009) Promoting axonal myelination for improving neurological recovery in spinal cord injury. *J Neurotrauma* 26: 1847-1856

Xiong Y, Rabchevsky AG, Hall ED (2007) Role of peroxynitrite in secondary oxidative damage after spinal cord injury. *J Neurochem* 100: 639-649

Yarkony GM, Katz RT, Wu YC (1986) Seizures secondary to autonomic dysreflexia. *Arch Phys Med Rehabil* 67: 834-835

Yozbatiran N, Berliner J, O'Malley MK, Pehlivan AU, Kadivar Z, Boake C, Francisco GE (2012) Robotic training and clinical assessment of upper extremity movements after spinal cord injury: a single case report. *J Rehabil Med* 44: 186-188

Zafra F, Ibanez I, Gimenez C (2017) Glycinergic transmission: glycine transporter GlyT2 in neuronal pathologies. *Neuronal Signal* 1: NS20160009

Zhang SX, Huang F, Gates M, Holmberg EG (2011) Scar ablation combined with LP/OEC transplantation promotes anatomical recovery and P0-positive myelination in chronically contused spinal cord of rats. *Brain Res* 1399: 1-14

Ziegler G, Grabher P, Thompson A, Altmann D, Hupp M, Ashburner J, Friston K, Weiskopf N, Curt A, Freund P (2018) Progressive neurodegeneration following spinal cord injury: Implications for clinical trials. *Neurology* 90: e1257-e1266

List of publications

Granier C, Schwarting J, Fourli E, Laage-Gaupp F, Hennrich AA, Schmalz A, Jacobi A, Wesolowski M, Conzelmann KK, Bareyre FM (2020) Formation of somatosensory detour circuits mediates functional recovery following dorsal column injury. *Sci Rep* 10: 10953